University of Denver

Digital Commons @ DU

1-1-2019

Control Strategy for a Small-Scale Microgrid Based on Battery Energy Storage System-Virtual Synchronous Generator (bess-Vsg)

Wei Gao
University of Denver

Recommended Citation

Control Strategy for a Small-Scale Microgrid Based on Battery Energy Storage System-Virtual Synchronous Generator (bess-Vsg)

Abstract

As one of widely deployed renewable energy resources, PV power is playing a very important role in microgrids today. It has advantages such as making the best of natural solar energy and being friendly to our environment. In this thesis, solar PV based microgrid is studied using modeling and simulation. Microgrid can run in either grid-connected-mode or islanded-mode. However, there are also some disadvantages for solar power. For solar panel, its output is influenced by weather conditions such as illumination intensity and temperature. In addition, during the control process of grid-connected mode, it is hard to guarantee its output power at the maximum power point all the time. In this thesis, the Maximum Power Point Tracking (MPPT) control for Solar PV energy is used. Besides, the frequency control is also a very important issue for guaranteeing the quality of the electricity in the microgrid. By using an effective way of BESS-VSG, which means Battery Energy Storage System-Virtual Synchronous Generator, the frequency can be controlled to the nominal value faster and more smoothly when there is a fluctuation in the PV power generation and/or load change, leading to higher stability and robustness.

This thesis focuses on the modeling and control of the PV and BESS-VSG system, and the proposed modeling and control method are verified in MATLAB/Simulink.

Document Type
Thesis

Degree Name
M.S.

Department
Electrical Engineering

First Advisor
David Wenzhong Gao, Ph.D.

Second Advisor
Yun-bo Yi, Ph.D.

Third Advisor
Mohammad Matin, Ph.D.

Keywords
Control, Microgrid, Power system, Renewable energy

Subject Categories
Electrical and Computer Engineering | Electrical and Electronics | Engineering | Power and Energy

Publication Statement

CONTROL STRATEGY FOR A SMALL-SCALE MIRCROGRID

BASED ON BATTERY ENERGY STORAGE SYSTEM-VIRTUAL SYNCHRONOUS

GENERATOR (BESS-VSG)

_____

A Thesis

Presented to

the Faculty of the Daniel Felix Ritchie School

of Engineering and Computer Science

University of Denver

_____

In Partial Fulfillment

of the Requirements for the Degree

Master of Science

_____

by

Wei Gao

November 2019

Advisor: Dr. David Wenzhong Gao

Author: Wei Gao
Title: CONTROL STRATEGY FOR A SMALL-SCALE MICROGRID BASED ON BATTERY ENERGY STORAGE SYSTEM-VIRTUAL SYNCHRONOUS GENERATOR (BESS-VSG)
Advisor: Dr. David Wenzhong Gao
Degree Date: November 2019

Abstract

As one of widely deployed renewable energy resources, PV power is playing a very important role in microgrids today. It has advantages such as making the best of natural solar energy and being friendly to our environment. In this thesis, solar PV based microgrid is studied using modeling and simulation. Microgrid can run in either grid-connected-mode or islanded-mode. However, there are also some disadvantages for solar power. For solar panel, its output is influenced by weather conditions such as illumination intensity and temperature. In addition, during the control process of grid-connected mode, it is hard to guarantee its output power at the maximum power point all the time. In this thesis, the Maximum Power Point Tracking (MPPT) control for Solar PV energy is used. Besides, the frequency control is also a very important issue for guaranteeing the quality of the electricity in the microgrid. By using an effective way of BESS-VSG, which means Battery Energy Storage System-Virtual Synchronous Generator, the frequency can be controlled to the nominal value faster and more smoothly when there is a fluctuation in the PV power generation and/or load change, leading to higher stability and robustness.

This thesis focuses on the modeling and control of the PV and BESS-VSG system, and the proposed modeling and control method are verified in MATLAB/Simulink.

Acknowledgements

I would like to thank all the people that helped me a lot during this period for my master thesis study.

Firstly, I very much appreciate my advisor Dr. David Wenzhong Gao for his diligent help including his advice and suggestions. Also, I am grateful for those tremendous experience that he provided for research, conference and internship during my study.

I am also grateful to the committee chair Dr. Yunbo Yi and committee member, Dr. Mohammad Matin. Thank you for taking time out of your busy schedule for helping my thesis and oral defense.

Specially, I would like to thank Dr. Margareta Stefanovic for her wonderful control classes that are very beneficial to me. Further, my thanks go to my labmates at University of Denver: Weihang Yan, Qiao Li, Abdullah Alharbi, Shruti Singh, Khawla Benjuma for their selfless assistance when I had problems in my work.

Last but not the least, I really appreciate my family for their continuous support for my academic study.

Table of Contents

List of Tables

List of Figures

Chapter One: Introduction

1.1 Concepts of Microgrid

Renewable energy has been paid more and more attention due to limited conventional fossil fuels. In addition, the environmental problem is also severe and urgent to be solved. According to the latest data from Energy Information Administration (EIA), the power output of renewable energy exceeds coal first time in the United States, which marks the arrival of the next generation of electricity.

In 2001, the concept of Microgrid was proposed by Consortium for Electric Reliability Technology Solutions (CERTS) for the first time. Since then, a lot of different definitions are created by different countries; however, a typical microgrid includes distributed powers generators (such as PV and wind power) and loads. It can provide the electricity and/or heat, connect and disconnect from the grid to run in either grid-connected mode or islanded mode [1] [2]. In order to achieve the goal, it needs smart switch and inverter controller to complete the synchronization with grid [3].

With a lot of Distributed Generators (DGs) as additional power supply in Microgrid, it has the following characteristics:

Flexibility: Since microgrid can run in either grid-connected mode or islanded mode, it is flexible to supply to or import power from the grid and can avoid its damage by disconnecting from the main grid when there is an event happening in the main grid.

Compatibility: As additional power supply in grid-connected mode, it can help balance the load demand during daily life, especially at the peak time when the power grid is not capable of meeting load demands.

Economy: Besides the benefits of using the natural energy as the resources of microgrid, those DGs can be built near to the location of the load to reduce the loss due to power flowing in transmission lines [4].

1.2 Control Strategies of Microgrid

There are several main control stratergies for microgrid: Master-Slave Control, Peer to Peer Control and Hierarchical Control.

1.2.1 Master-Slave Control

In islanded mode, one of the DGs acts as the swing bus and decides the nominal voltage

and frequency, and all other DGs use constant power control based on this specific voltage

and frequency [5]. The structure of this mode is shown as below:
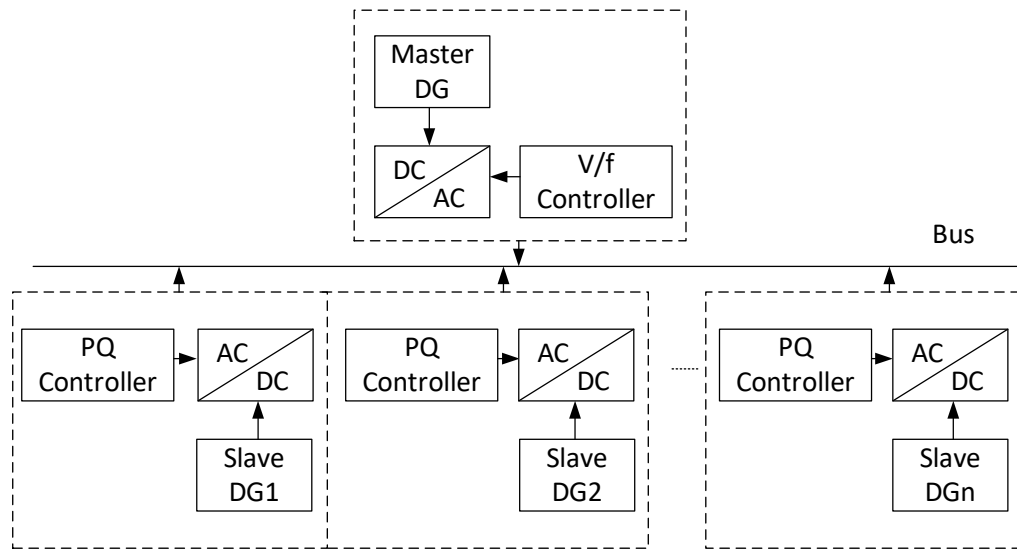
Figure 1.1 The structure of Master-Slave Control mode for Microgrid

1.2.2 Peer to Peer Control

In this mode, DGs are equal, so there is no master and slave anymore. Each DG

controls its voltage and frequency based on the information from the common bus. The

most common controller for them is Droop Controller, which can change their own power

to share the loads based on different droop coefficients [6]. The structure of this mode is

shown as below:
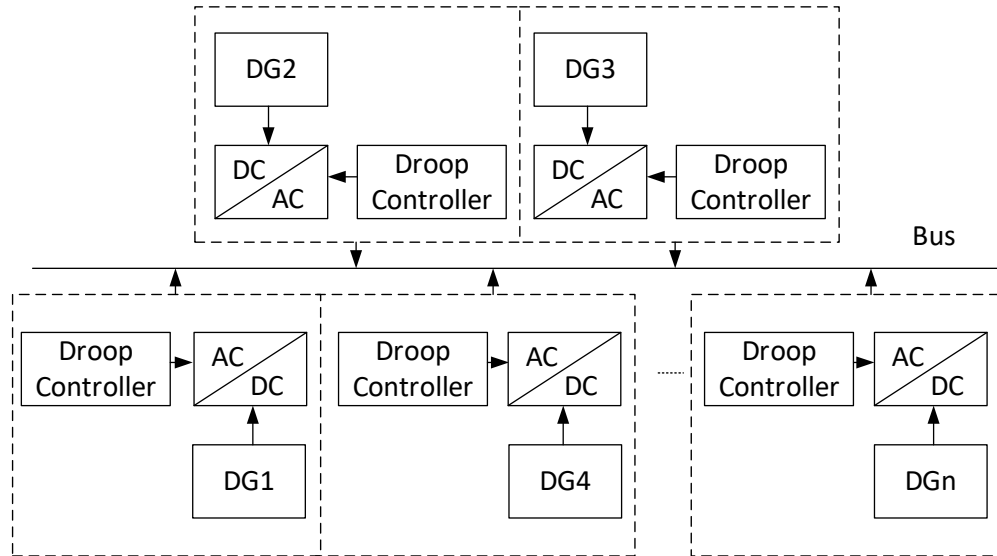
Figure 1.2 The structure of Peer to Peer Control mode for Microgrid

This mode relies on the reasonable droop coefficients, and after that, it is easy and

convenient for each DG to function in a plug-and-play fashion because there is no need to

have communication between those DGs. They can share the changes due to the varying

loads and then facilitate the system to reach at a new stable point. But there is a difference

between the new stable point and the old stable point.

1.2.3 Hierarchical Control

A common application of the Hierarchical Control is the power economic dispatch for the advanced control. In recent years, optimization is more and more important in the power economic dispatch such as optiamal power flow (OPF) and disturbuted optimal energy management. In [7], the distributed optimal multi-agent energy management based on Newton-Raphson method is proposed; specifically in [8], [9], the proposed Newton-Raphson based corridination algorithm can solve the current complex optimation problem in multienergy system very fast. Typically, in the Hierarchical Control, there is a central control unit, which can send the control information to each DG, then those DGs can control themselves to obtain the goal based on different control commands. During this process, the central control unit is the core of the whole system, which needs to collect electrical information all the time and then makes schedule for next step [10]. The structure of this mode is shown as below:
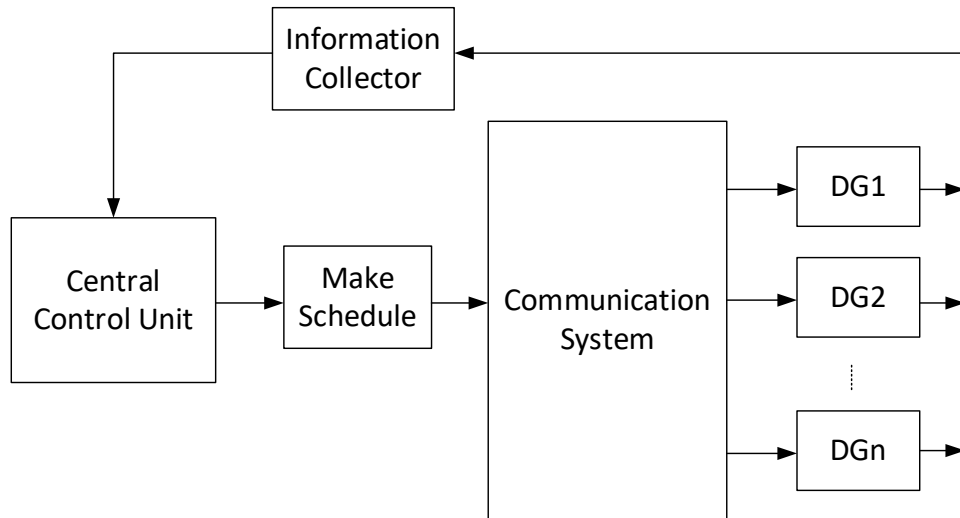
Figure 1.3 The structure of Hierarchical Control mode for Microgrid

All the controllers of DGs have been explained in the previous two modes for different purposes. This mode is the most intelligent and manageable, but it costs most and is most complicated. With this advanced mode, the microgrid can be more methodical in applications.

1.3 Literature Review

With a high penetration of renewable energy resources, the issues of frequency stability will occur gradually. More specifically, in Microgrid, lots of renewable energy generators replace the traditional generators and result in insufficient capacity for primary/secondary

control, leading to frequency fluctuation of the microgrid due to the uncertainty of renewable energy [11]. Furthermore, the whole system is losing inertia because power electronics based generators do not provide natural inertia [12]. The low inertia will cause the microgrid to be more sensitive to the disturbance and thus a small load change may result in a serve deviation in frequency, which decreases the stability of the microgrid [13].

In order to reduce these disadvantages, the concept of Virtual Synchronous Generator (VSG) is proposed [14]. The VSG technique can mimic the characteristics of the traditional synchronous generators with damping and inertia by using appropriate control algorithm. A complete VSG model with consideration of mechanical and electromagnetic transient state is proposed in [15]. Also, considering distributed cooperative control for distributed renewable energy, some distributed secondary control of VSG for Microgrid can be referred to [16], [17]. Specifically, VSG has inherent advantage for wind turbine because of the stored energy in the blades of the wind turbine and thus does not need the battery necessarily to exchange energy during the operation of VSG. In [18], it introduces the main popular methods for variable speed wind turbines (VSWTs). Furthermore, multiple virtual rotating masses of VSG for permanent magnet synchronous generator-variable speed wind

turbine generators (PMSG-WTG) is proposed in [19]. Many other applications of VSG with grid-connected mode and islanded mode for microgrid are introduced in [20] [21] [22].

1.4 Expected Contribution

This thesis aims to design and build a small-scale microgrid model in MATLAB/Simulink and verify the proposed VSG control method in this model. The modeling and control work aim to achieve the following contributions:

1. Building and verifying the MPPT controller for PV system with fluctuation.

2. Implementing a working test platform for small-scale microgrid with stable and nominal frequency and voltage.

3. Showing that the microgrid can run in either grid-connected mode or islanded mode.

4. Verifying the better performance of the proposed Alternating VSG algorithm for the frequency control of the microgrid.

Chapter two: PV Related Control

2.1 PV Modeling

During the development of PV system in recent years, there are lots of different types of PV modeling such as single diode model and double diode models. A comparison between different electrical mathematical models is provided in [23].

2.1.1 Single diode model for PV Cell

Basically, a PV cell is a special type of p-n junction, which is embedded in a thin wafer of semiconductor such as silicon. The principle of energy conversion is the photovoltaic phenomenon, which converts solar radiation to electricity. For those photons with higher energy than the band-gap energy of the semiconductor, they can help generate some free electron-hole pairs in the semiconductor. With the internal electric fields, those electron-hole pairs will be attracted or excluded to two sides respectively, and thus the photocurrent appears. Due to the nonlinearity of the I-V and P-V characteristics under variable irradiance and temperature, usually it needs to be linearized in small-signal analysis [24].

The equivalent electrical mathematical model is shown as following for ideal, simplified and practical model, respectively:
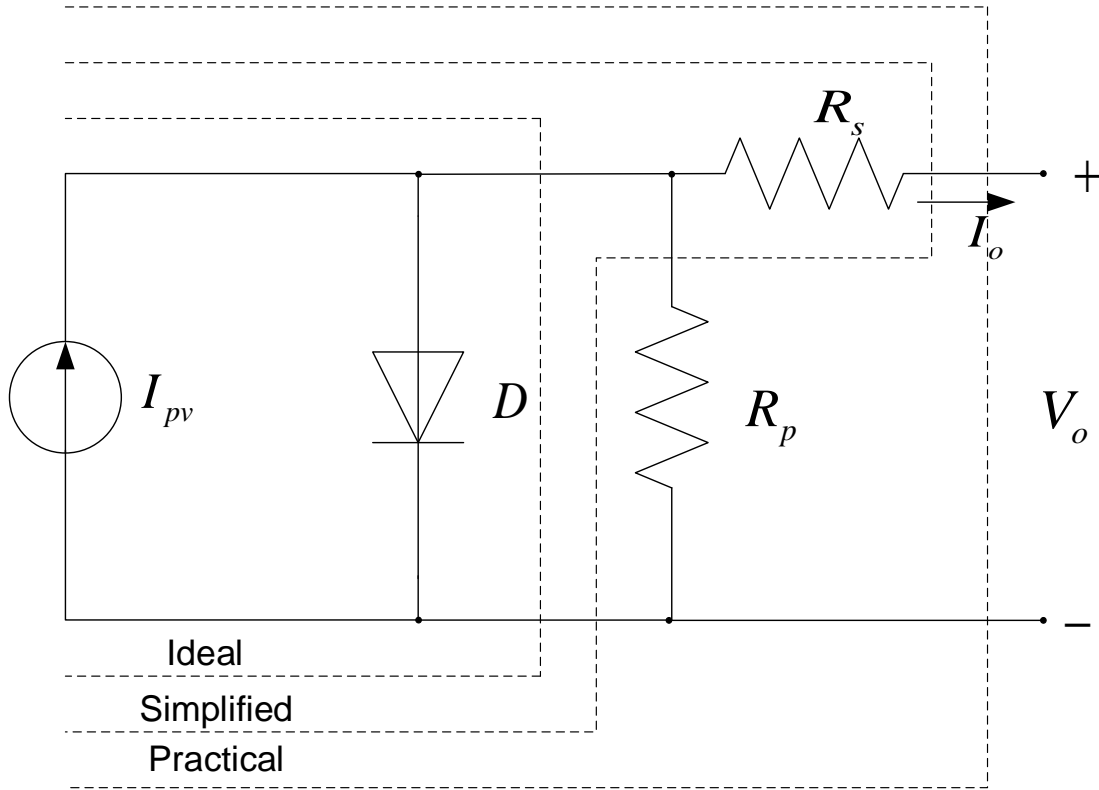
Figure 2.1 Three different equivalent circuits with different scenarios

For practical model, it consists of an ideal current source I_{pv} and a diode D, a parallel resistor R_p modeling a leakage current, and a series resistor R_s representing an internal resistance. Based on the circuit structure and Kirchhoff's law, the I-V characteristic can be expressed as below:

$$I_o = I_{pv} - I_s[\exp\left(\frac{q(V_o + I_o R_s)}{kT_c A}\right) - 1] \tag{2.1}$$

10

where, I_o and V_o are the output current and the output voltage of this PV cell respectively; I_{pv} is the photocurrent of this PV cell; I_s is the diode reverse saturation current; $q = 1.69 \times 10^{-19}C$ is an electron charge; $k = 1.38 \times 10^{-23}J/K$ is the Boltzmann's constant; T_c is the temperature of this PV cell in Kelvin; and A is the ideal factor. In addition, the photocurrent I_{pv} is usually related to the solar radiation and the working temperature of the PV cell, which can be expressed as below:

$$I_{pv} = I_{sc} + K_I(T_c - T_0)H \tag{2.2}$$

where, I_{sc} is the short-circuit current at reference temperature $T_0 = 25°C$ and the reference irradiance $1kW/m^2$, K_I is the temperature coefficient of its short circuit current and H is the solar irradiation in kW/m^2. Besides, the relationship between the diode reverse saturation current and the cell temperature is given:

$$I_s = I_{rs}(T_c/T_0)^3 \exp[qE_g(1/T_0 - 1/T_c)/kA] \tag{2.3}$$

where I_{rs} is the reverse saturation current of this cell at reference temperature and solar radiation, E_g is the band-gap energy for the semiconductor. For ideal factor A, it is different for different materials, which are given as [25]:

Table 2.1 Different ideal factor A for on different semiconductor materials

Semiconductor Material	A
Si-mono	1.2
Si-poly	1.3
a-Si:H	1.8
a-Si:H tandem	3.3
a-Si:H triple	5
CdTe	1.5
CIS	1.5
AsGa	1.3

2.1.2 Single diode model for PV Module and Array

A single PV cell is not enough because each cell's power is usually less than 2W at about 0.5V. Thus, many PV cells should be connected in series or parallel way to obtain a higher power. Assume that there are N_s cells in series and N_p cells in parallel. Then the equivalent electrical model is given as below:
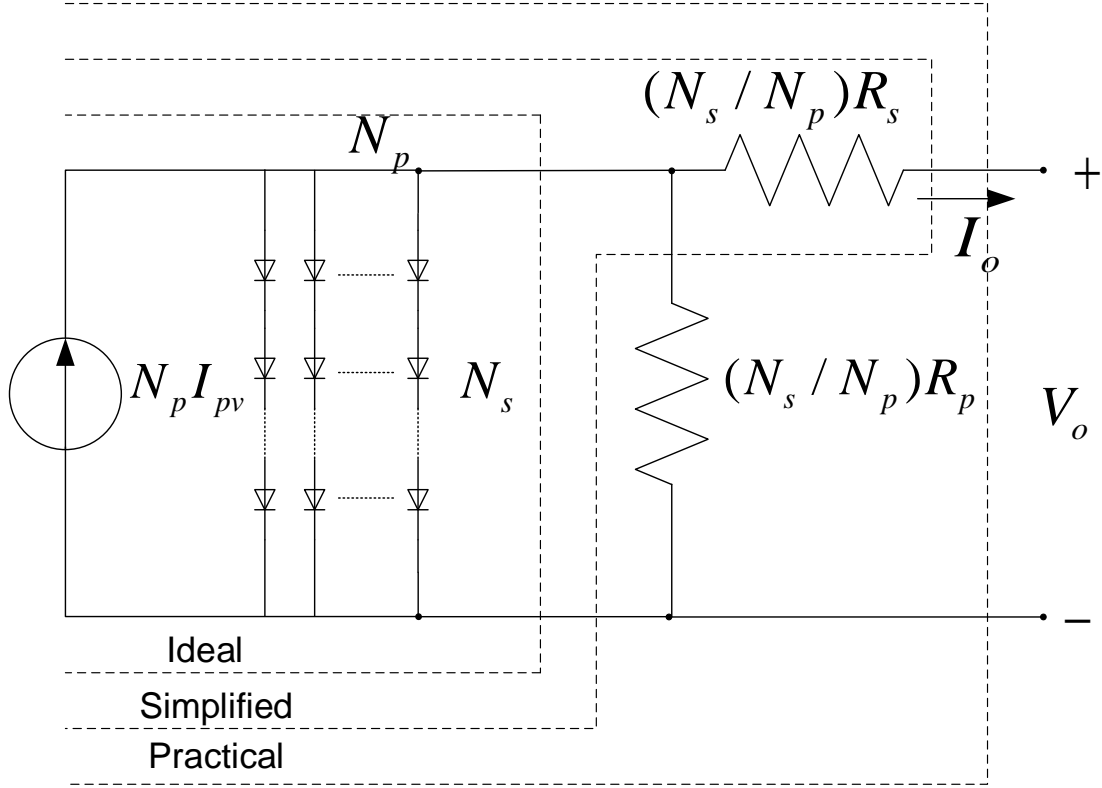
Figure 2.2 Three different equivalent circuits of a PV module

In this way, the V-I characteristic of this PV module can be expressed as below [26]:

$$I_o = N_p I_{pv} - N_p I_s [\exp\left(\frac{q(N_p V_o + N_s I_o R_s)}{N_p N_s k T_c A}\right) - 1]$$ (2.4)

2.1.3 Double diode model for PV Cell

In order to obtain more detailed dynamics of the p-n junction, the double diode model is proposed, which includes another diode in parallel with the original diode. The equivalent circuit is shown as below [27]:

13
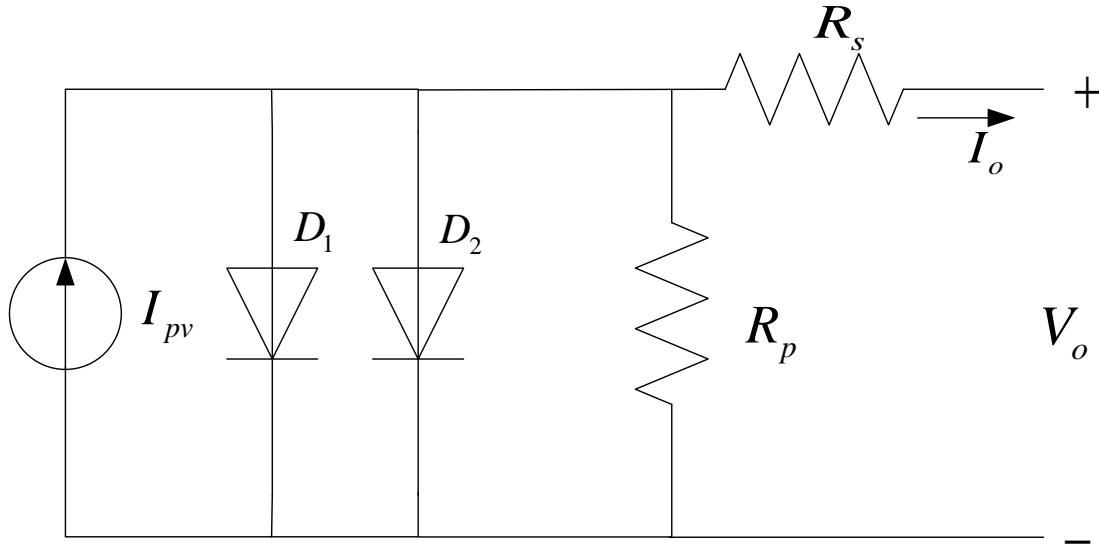
Figure 2.3 The equivalent circuit of a double diode model for PV Cell

The V-I characteristic can be obtained based on the following function:

$$I_o = I_{pv} - I_{s1}\left[\exp\left(\frac{q(V_o+I_oR_s)}{kT_cA}\right) - 1\right] - I_{s2}\left[\exp\left(\frac{q(V_o+I_oR_s)}{kT_cA}\right) - 1\right] \qquad (2.5)$$

where, I_{s1} is the diode D_1's reverse saturation current; I_{s2} is the diode D_2's reverse saturation current and all other parameters are the same as explained in the single diode model.

2.1.4 Double diode model for PV Module and Array

Similar to single diode model for PV Module and Array in Section 2.1.2, the mathematical equation is derived as below:

$$I_o = N_p I_{pv} - N_p I_{s1} \left[\exp \left(\frac{q(N_p V_o + N_s I_o R_s)}{N_p N_s k T_c A} \right) - 1 \right] - N_p I_{s2} \left[\exp \left(\frac{q(N_p V_o + N_s I_o R_s)}{N_p N_s k T_c A} \right) - 1 \right] (2.6)$$

2.2 Maximum Power Point Tracking (MPPT)

For PV system, the output power is dependent on the circuit structure, solar radiation and temperature, so the Maximum Power Point Tracking (MPPT) is necessary for a PV system to optimize the utilization of the solar cells constantly [28] [29]. With the development of PV system in recent years, a lot of methods have been proposed for MPPT such as fractional open-circuit voltage and short-circuit current [30], the fuzzy logic control [31] and the Artificial Neural Network (ANN) [32]. The most popular methods include perturb and observe method (P&O) [33], the incremental conductance method (INC) and the hill climbing method (HC) [34]. Due to the relatively easier implementation, the last three methods are widely used, and this thesis uses P&O method with more details shown in Chapter 3. Those methods are described in the following subsections. Before introducing those MPPT methods, the I-V characteristic curve of PV cells should be given and explained.

2.2.1 I-V and P-V Characteristic Curves of a PV Module and Array

The I-V curve and P-V curve of a typical PV Array can be obtained by programming the aforementioned mathematical model in MATLAB/Simulink. For a specific Module SunPower SPR-305E-WHT-D, the following figures can be generated:
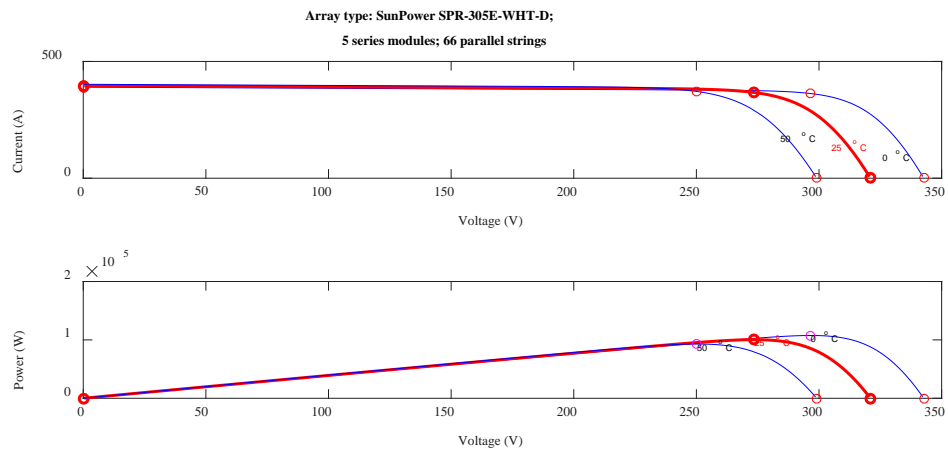
Figure 2.4 The I-V and P-V curves of the PV Array

Assume that the cell temperature is $25°C$, then the red point in the I-V curve represents the Maximum Power Point (MPP), which corresponds to the red MPP in the P-V curve. It can also be seen that the short-circuit current increases and the open-circuit voltage decreases as the cell temperature rises. This means that the maximum power becomes smaller as cell temperature increases; however, the enhancement of the solar

16

radiation will increase both short-circuit current and open-circuit voltage so that the maximum power becomes larger [35].

2.2.2 Perturb and Observe Method (P&O)

The principle of this technique is to perturb PV module operating voltage periodically with a small increment, then observe the change direction of the output power so that the further control signal can be determined. For example, in combination with the P-V characteristic curve, if the output power increases after voltage increases, then the working voltage should be kept increasing in the same direction until output power does not increase anymore indicating MPP is reached; otherwise it should be changed in the opposite direction. P&O algorithm has its advantage with only measuring the voltage and current of the PV module. The flowchart of this algorithm is shown below:
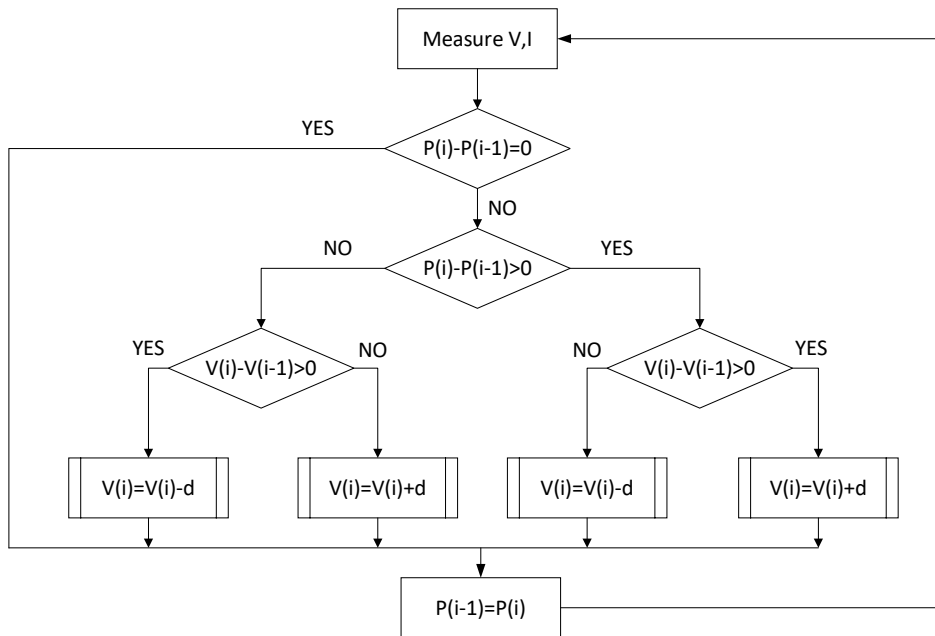
Figure 2.5 The flowchart of the P&O algorithm

where, P(i) is the output power of the i-th iteration; d is the step size of working voltage change for this PV module.

2.2.3 Incremental Conductance Method (INC)

From the Ohm's law, we know:

$$P = VI \tag{2.7}$$

At the Maximum Power Point, (2.8) should be hold:

$$\frac{dP}{dV} = I + V\frac{dI}{dV} = 0 \tag{2.8}$$

For a practical application, it can be written as:

$$I + V\frac{\Delta I}{\Delta V} = 0 \qquad\qquad (2.9)$$

where, ΔI and ΔV are small increments of current and voltage, respectively. The term $\frac{\Delta I}{\Delta V}$ is called incremental conductance, from which this MPPT technique is named. This method is easy to be implemented like the P&O method, so it is also widely used in industry. The flowchart of this algorithm is shown as below:
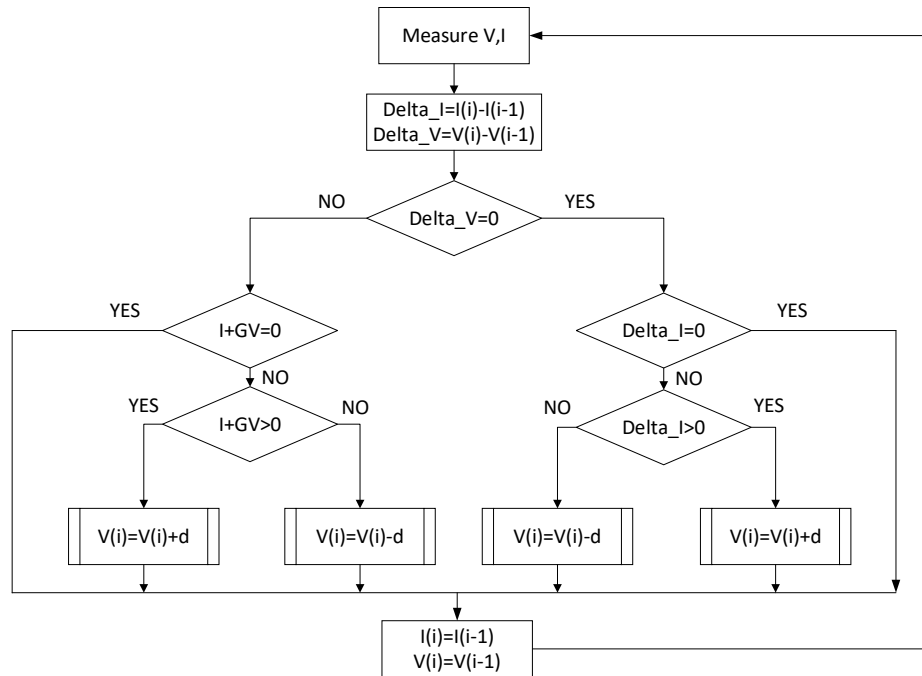
Figure 2.6 The flowchart of the INC algorithm

In Figure 2.6, G is the incremental conductance $\frac{\Delta I}{\Delta V}$; all other parameters have been stated in the P&O algorithm.

2.2.4 Hill Climbing Method (HC)

This technique is always combined with boost converter so that the duty cycle can be changed to find the maximum power point. Firstly, if $dP/dD = 0$, then it indicates that the maximum power point is tracked, which means that the difference of the output power between the present time step and the previous time step determines the value of the duty cycle in each sampling period. Secondly, if $dP > 0$, then the duty cycle needs to be increased; otherwise the duty cycle needs to be decreased. The main idea is to change the equivalent circuit parameters by controlling the boost converter connected with the PV module. The flowchart is shown as below:

```
                    ┌──────────────┐
              ┌────▶│  Measure V,I │◀──────────────┐
              │     └──────────────┘               │
              │            │                        │
              │            ▼                        │
              │     ┌──────────────┐               │
              │     │  P(i)=V(i)I(i)│               │
              │     └──────────────┘               │
              │            │                        │
         NO   │            ▼              YES       │
         ┌────┴───◀─◇ P(i)-P(i-1)>0 ◇──────▶┐      │
         ▼                                   ▼      │
  ┌──────────────┐                    ┌──────────────┐
  │  D(i)=D(i)-d │                    │  D(i)=D(i)+d │
  └──────────────┘                    └──────────────┘
         │            ┌──────────────┐        │      │
         └──────────▶│System Running│◀───────┘      │
                      └──────────────┘               │
                             │                        │
                             ▼                        │
                      ┌──────────────┐               │
                      │  I(i)=I(i-1) │───────────────┘
                      │  V(i)=V(i-1) │
                      └──────────────┘
```
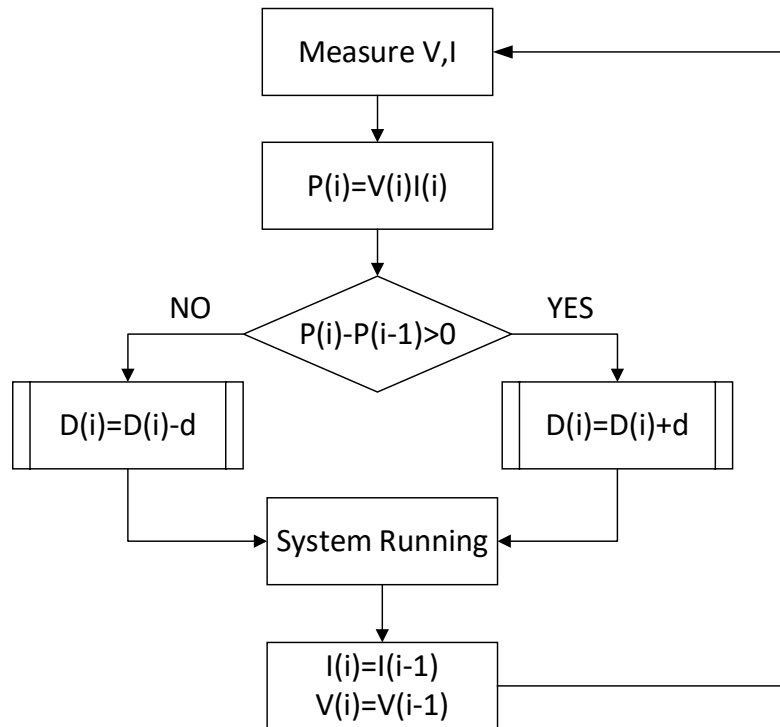
Figure 2.7 The flowchart of the HC algorithm

2.3 Inverter Controller of PV Grid-connected System

As a DC source, PV needs to be converted to AC source by power electronics converters in order to be connected to grid. In addition to the MPPT control for PV module, grid-connected control is also necessary for a PV grid-connected system to enable the entire PV system to be more efficient and stable. Two typical PV converter systems for grid connection are monopolar type and two-stage type. The former one is cheaper and more

efficient, and the latter one is easier to implement [35]. The difference between the

monopolar type and the two-stage type is that the two-stage type goes through a DC-DC

Boost converter first, then connects with a DC-AC converter; however, the monopolar type

does not have the DC-DC Boost converter. Here in this thesis, the two-stage type is

introduced and used. The block diagram and the electrical diagram of this type PV system

are shown as below:
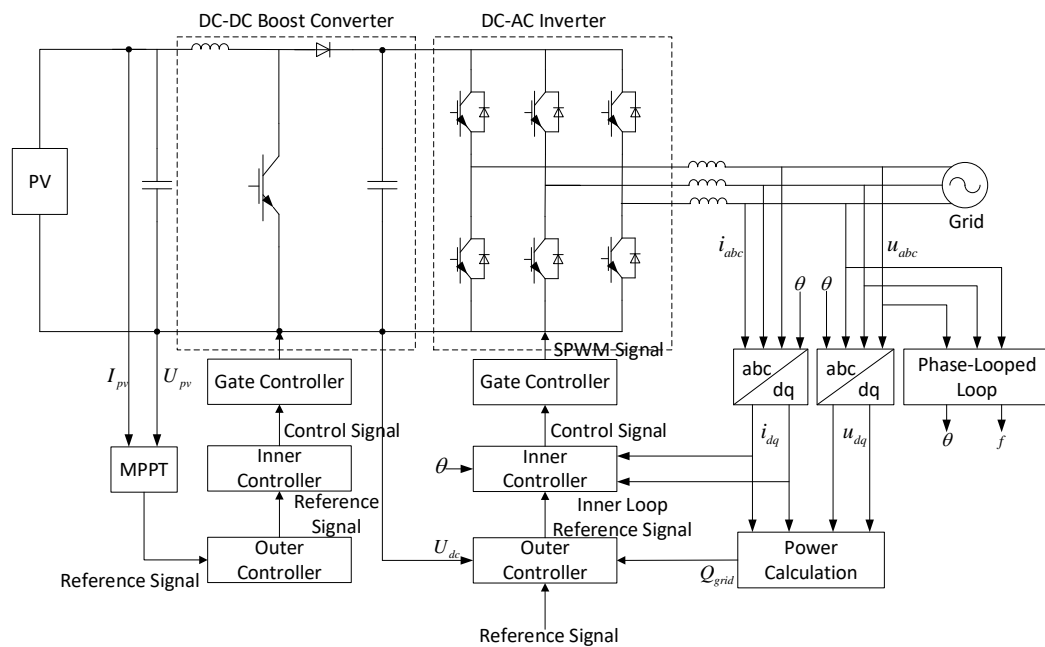
Figure 2.8 The electrical diagram of the two-stage type PV grid-connected system

The typical inverter control technique includes outer loop control and inner loop

control as shown in Figure 2.8.

In addition to the DC-Voltage and Reactive Power Control for outer loop, the details of some other outer loop control techniques are also explained in the following subsections.

2.3.1 Outer Loop Control

Several outer loop controls have been proposed for different purposes. [36] [37] explained the grid-connected control mode (P/Q Control) and voltage-frequency control mode (V/f Control). The traditional and advanced Droop Control are introduced in [38] [39] [40]. The detail of each technique is given in the following subsections.

1) Constant Power Control (P/Q Control)

The aim of this technique is to control the real power and reactive power of the DG output power to follow the reference power, and the principle is to control the decoupled real power and reactive power individually. The control structure is shown as below:
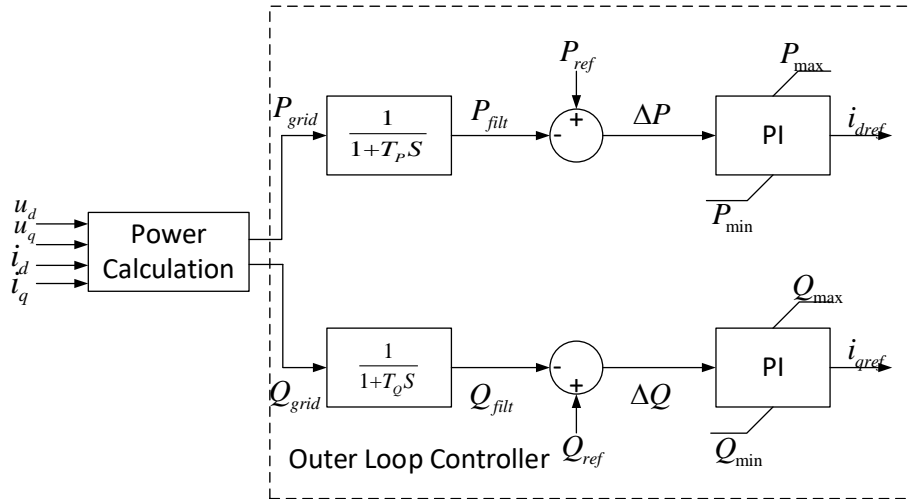
Figure 2.9 The PQ Control structure of outer loop for DG

However, this controller cannot maintain the frequency and voltage constant. This

situation is illustrated from the following curves [41]:
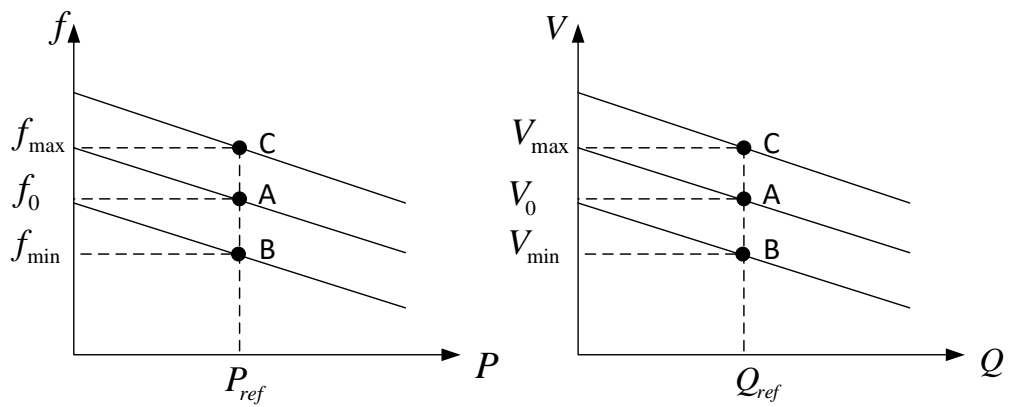
Figure 2.10 The schematic diagram of the PQ Control

Assume that the operating point is A at initial time, and the load demand is P_{ref} and

Q_{ref}. At the moment, the output power of the DG is also P_{ref} and Q_{ref}, so the system is

balanced with the system frequency f_0 and the system voltage V_0. If the load demand

increases, the system frequency will decrease to f_{min} because of the constant output real

and reactive power of DG; otherwise the running point will go to point C. All the scenarios

should be considered that the system frequency and system voltage should be in the range

$f_{min} < f < f_{max}$ and $V_{min} < V < V_{max}$, respectively.

2) Constant Voltage/Constant Frequency Control (V/f Control)

Similar to Constant Power Control, V/f Control is to maintain the voltage and

frequency of the system constant and stable despite the variable output power of the DG.

The control structure is shown as below:
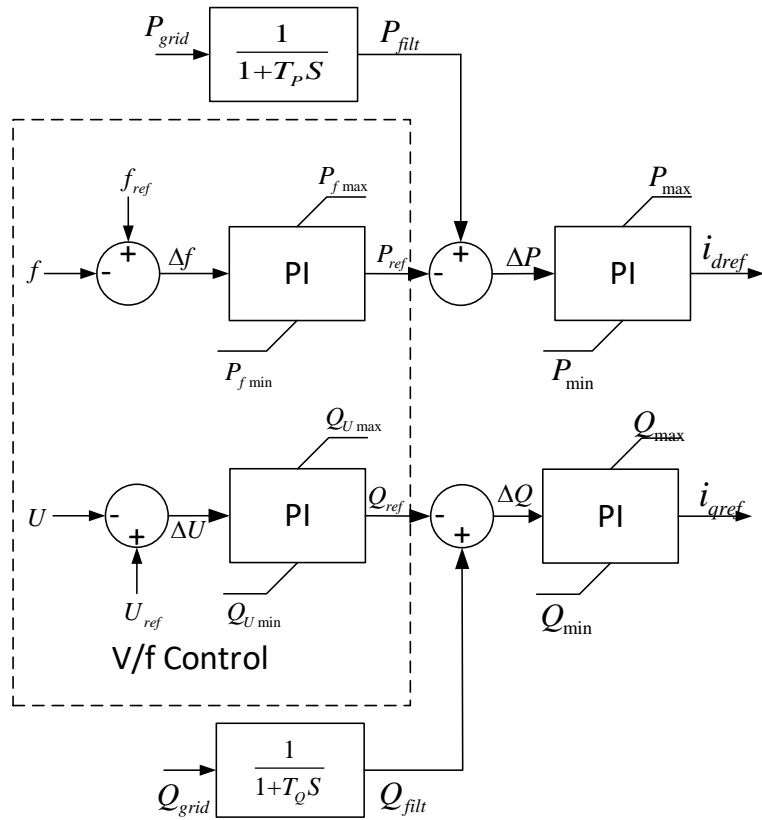
Figure 2.11 The V/f Control structure of outer loop for DG

And the principle of this control can be illustrated from the following curve:
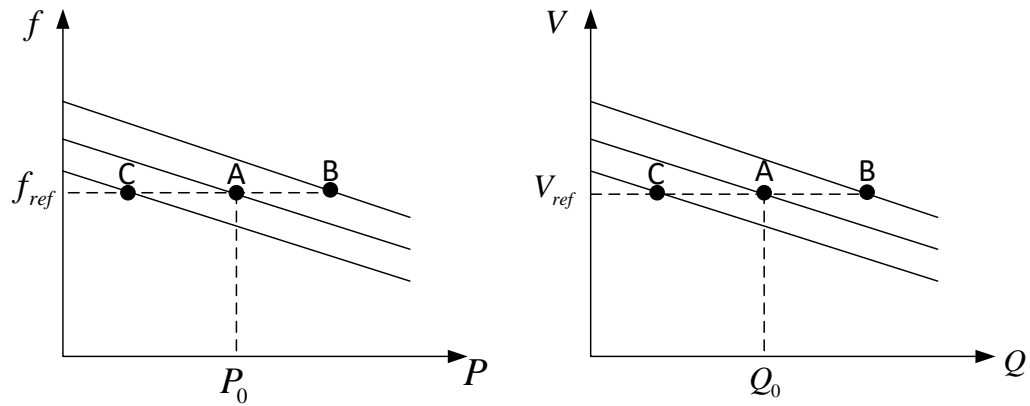
Figure 2.12 The schematic diagram of the V/f Control

As the curve shows, the operating point will move in the dotted line when the load changes, so with the voltage and frequency control, it can guarantee the frequency and voltage are nominal. This control method is mainly used in islanded mode because the microgrid system frequency and voltage are dependent on the power output of DGs in this mode. In other words, one of the DGs may function as the dominant generation like the swing bus in the traditional grid. However, since there is only DG to maintain the voltage and frequency, the balance between the load and the generation should be almost matched; otherwise the islanded microgrid is prone to be unstable.

3) Droop Control

This method is to mimic the characteristic of the traditional generator unit to assign each DG's output power according to each DG's capability to accommodate the new load

changes. There are two different basic Droop Control techniques: f-P and U-Q Droop

Control, P-f and Q-U Droop Control. The ideas are similar for these two types. Here, the

f-P and U-Q Droop Control structure is given:
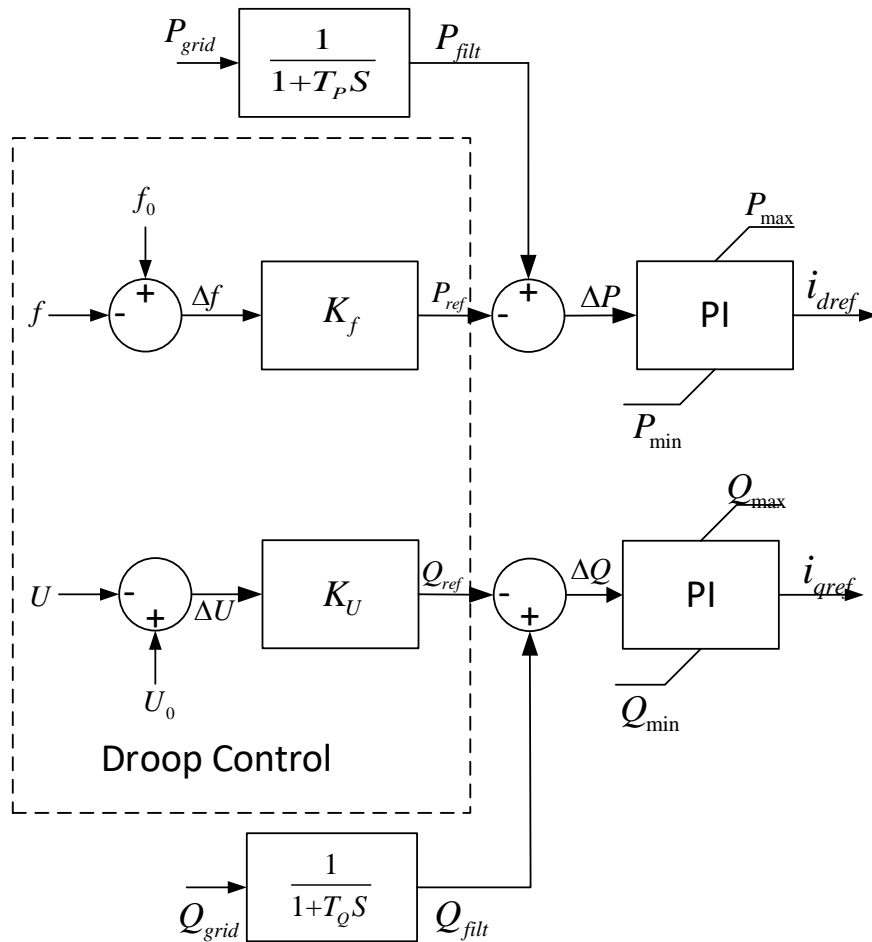
Figure 2.13 The Droop Control structure of the outer loop for DG

In this way, the difference between the Droop Control and the V/f Control is just the

different way of generating the power reference signal. However, both parameters of the

controllers need to be set properly to stabilize the system, and the Droop Control

Parameters K_f and K_U can be approximately calculated based on the system capacity.

The principle of this control can be illustrated from the following curve:
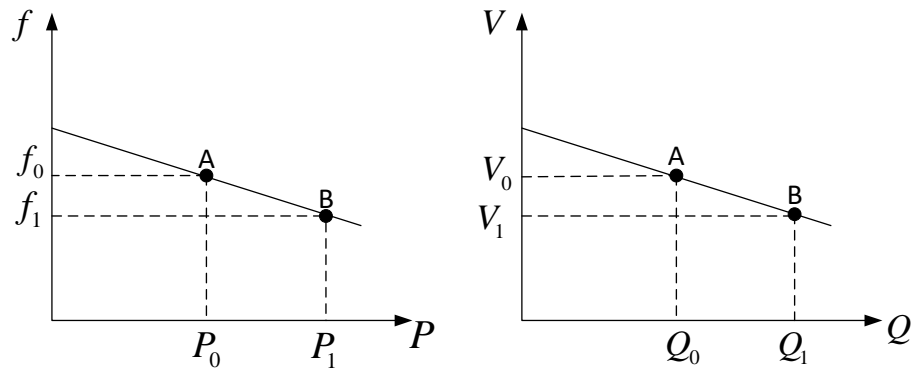
Figure 2.14 The schematic diagram of the Droop Control

Assume that the operating point is point A initially, and the frequency and voltage are

f_0 and V_0 respectively. Now, suppose that the load increases from P_0 to P_1, then the

frequency will decrease from f_0 to f_1 along the line. In the meantime, the load will also

decrease lightly because of the decreasing frequency. Finally, the operating point will be

stable at the new operating point B with the cooperation of the Droop Control and the load

self-regulating effect [42]. And the relationship between the P and f and Q and U are be

given as in (2.10), (2.11), respectively:

$$P = P_0 + (f_0 - f)K_f \tag{2.10}$$

$$Q = Q_0 + (U_0 - U)K_U \tag{2.11}$$

In addition, there are some other Droop Control methods, such as Virtual Impedance Method by using the characteristic of Q-L to mimic the characteristic of Q-U and P-U [43] [44] and Q-f control method by considering the characteristic of impendence in a low voltage distribution line [45].

2.3.2 Inner Loop Control

The purpose of the inner loop control is to guarantee the accurate control from the outer loop reference signals, and this is also reasonable from the control viewpoint because this is a closed dual-loop system based on the combination of outer loop and inner loop. It is basically a decoupling control based on different coordinate systems: $dq0$ rotating coordinate system, $\alpha\beta0$ static coordinate system and abc natural coordinate system. Here the most common $dq0$ rotating coordinate system is introduced due to its simplicity and convenience.

$dq0$ rotating coordinate system:

Based on the Park transformation, with in $dq0$ rotating coordinate system, three phase instantaneous signals can be transformed to $dq0$ two phase signals. The advantage is that

the transformed signal is DC signal instead of AC signal, and the structure of this inner

loop can be shown as below:
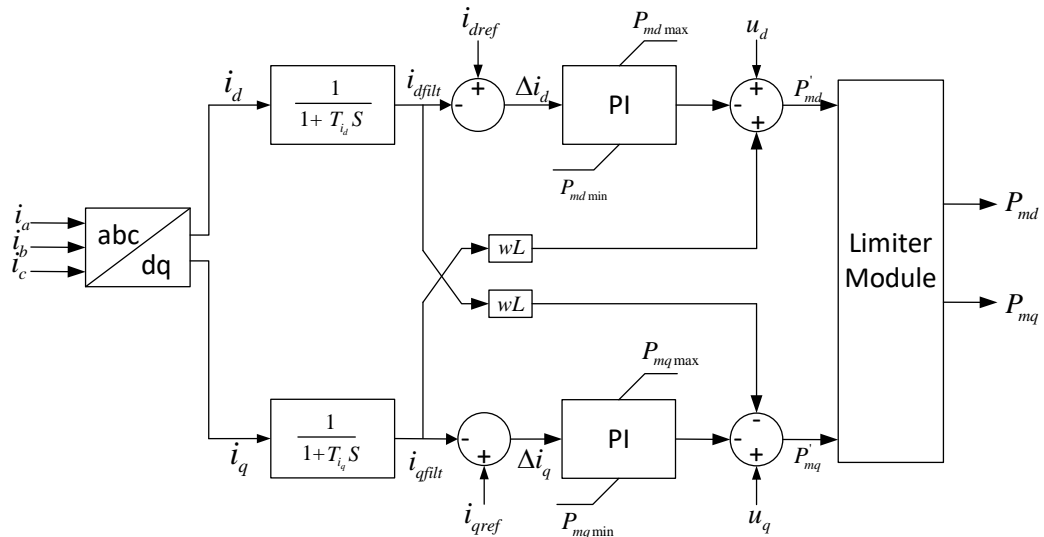
Figure 2.15 The typical control structure of the dq0 inner loop

As can be seen in Figure 2.15, the instantaneous current i_{abc} is transformed to i_{dq}

by the block abc/dq, and then through a lowpass filter. A PI controller can realize the

floating control. In the meantime, a dq decoupling control is used to control d and q

components respectively. With the limiter module, the inverter can operate within a linear

region, and the modulating signal is obtained finally.

2.3.3 Phase-Locked-Loop (PLL)

One popular application for PLL is to obtain the phase of the signal in power system, and it is necessary for transformation of coordinates such as from abc to dq0. The principle of PLL and more details can be referenced in [46]-[49].

The basic structure of PLL is shown as below:
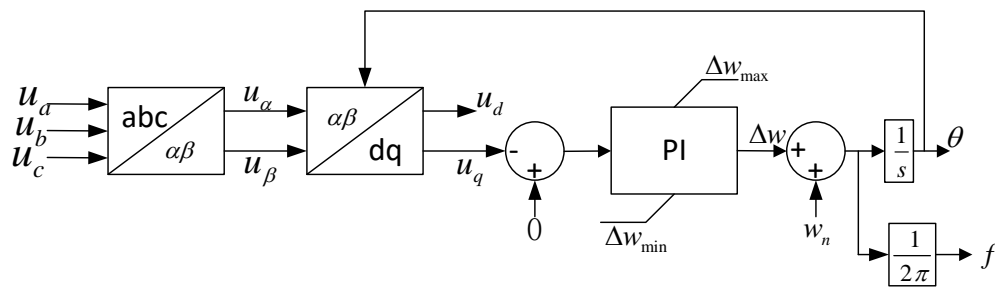
Figure 2.16 The typical structure of PLL

The overall goal of this PLL is to output the frequency and phase as the input signal.

Chapter Three: BESS-VSG Control System

The penetration of renewable energy is increasing rapidly in recent years in the United States. According the latest data from EIA (Energy Information Administration), the output of renewable energy exceeds coal first time in the United States. In particular, PV (photovoltaic) system plays a very important role in renewable energy.

However, PV systems are usually controlled by power electronic devices, which do not have much inertia as traditional power systems [50]. That is to say, the frequency is sensitive to vary if there is a fluctuation in load demand or generation, which is very unbeneficial to the system [51]. One method to stabilize frequency is the technique of Virtual Synchronous Generator (VSG), which can mimic the characteristic of the traditional synchronous generator with enough inertia so that the problem of frequency fluctuation can be alleviated [52]-[55].

3.1 Basic VSG Algorithm

As proposed, the principle of VSG algorithm is to mimic the characteristic of the traditional synchronous generator. VSG algorithm is based on the swing equation of the

synchronous generator. The VSG mathematical model is implemented by using control

blocks. The swing equation is shown as below:

$$P_{in} - P_{out} = J\omega\frac{d\omega}{dt} + D\Delta\omega \tag{3.1}$$

where, P_{in} is the input power of the synchronous generator; P_{out} is the

electromagnetic power of the stator; J is the moment of inertia; ω is the rotor angular

velocity; D is the damping coefficient; and $\Delta\omega = \omega - \omega_0$; ω_0 is the reference grid

angular velocity, which is $2\pi60$ in the United States. With the same idea, VSG algorithm

has the same formula:

$$P_{in} - P_{out} = J\omega_{vsg}\frac{d\omega_{vsg}}{dt} + D\Delta\omega \tag{3.2}$$

where, ω_{vsg} is the virtual angular velocity of the VSG; $\Delta\omega = \omega_{vsg} - \omega_0$; and all

other parameters have been explained in equation (3.1).

Since $\omega_{vsg} \approx \omega_0$, we can obtain:

$$P_{in} - P_{out} = J\omega_0\frac{d\omega_{vsg}}{dt} + D\Delta\omega \tag{3.3}$$

Here, by using Laplace Transformation on equation (3.3), the following is obtained:

$$P_{in} - P_{out} = J\omega_0\omega_{vsg}s + D(\omega_{vsg} - \omega_0) \tag{3.4}$$

Since this is a nonlinear system, it can be linearized at the operation point:

$$P_{in} - P_{out} = J\omega_0 s\omega_{vsg} + D(\omega_{vsg} - \omega_0) \tag{3.5}$$

Based on this equation, the control blocks can be created as follows:
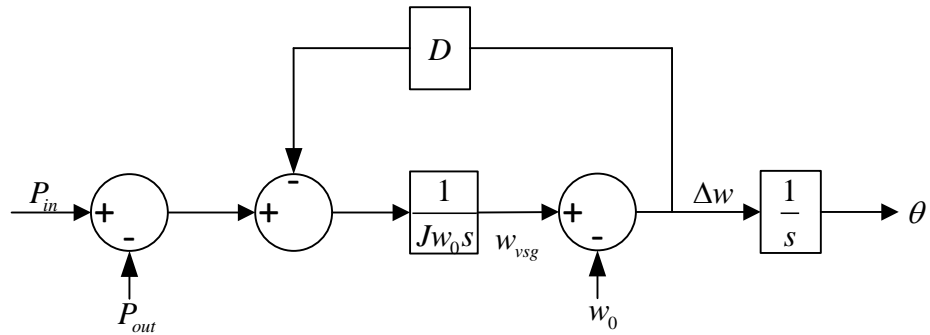
Figure 3.1 The structure of VSG algorithm

Beside the active power VSG algorithm, the reactive power or voltage also needs to be controlled. The typical control method is the Droop Control as discussed in the previous chapter. After both control signals from real power VSG control and reactive/voltage control are obtained, they can further be combined and used in the subsequent PWM/SPWM section.

3.2 Battery System for Energy Supply

Since the PV panel is controlled to output the maximum power by MPPT technique, extra energy needed for VSG algorithm is needed. Battery system can be combined with VSG algorithm to supply the needed energy. Many different batteries can be used for storage system, such as Nickel Cadmium (Ni-Cd), Nickel Metal Hydride (Ni-MH), Lithium Ion (Li-ion) and so on. Li-ion is mature and convenient, so Li-ion is used in this

thesis. [56] proposed a general charging/discharging model through curve-fitting method. In addition, different charging strategies such as Constant Current Charging, Voltage Limiting Charging, Floating Voltage Charging, Multi-stage Charging are introduced in [57]. And the discharging strategy is dependent on the situation, usually related to the system structure. Since the battery system is connected to the grid through inverter, the control method is similar to the inverter control as described in previous chapter.

3.3 Alternating VSG Algorithm

Since the performance of the frequency regulation is directly related to the moment of inertia, the characteristic can be changed if the moment of inertia is changing during the system operation [58]. One method of alternating moment of inertia and the is introduced in [59].

The typical power-angle curve for power system is shown as below:
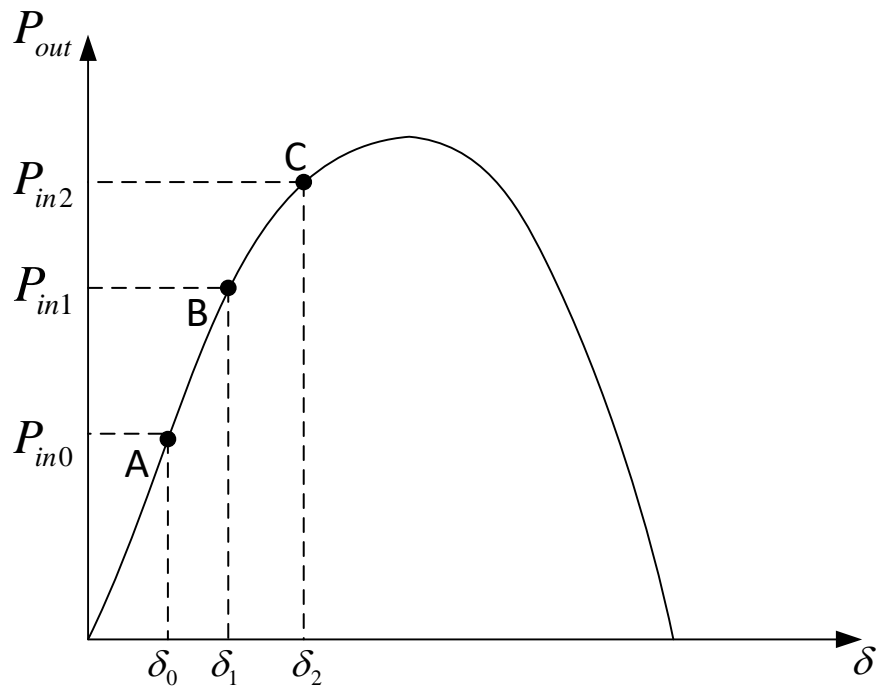
Figure 3.2 The typical power-angle curve of a synchronous generator

Assume that the system is operating at point A initially, and it is stable. For example, if the input power increases to point B, P_{in1}, the operating point will follow the curve from A to B, because the load is increasing as frequency increases. In this period, $\Delta\omega > 0$, and $d\omega_{vsg}/dt > 0$, it is defined as an acceleration segment. However, the goal is to alleviate the oscillation of the frequency when the load or generation changes. In this way, a big J can be used to reduce the acceleration; otherwise a small J should be used. And the ideal step response of frequency for alternating inertia is shown as below:
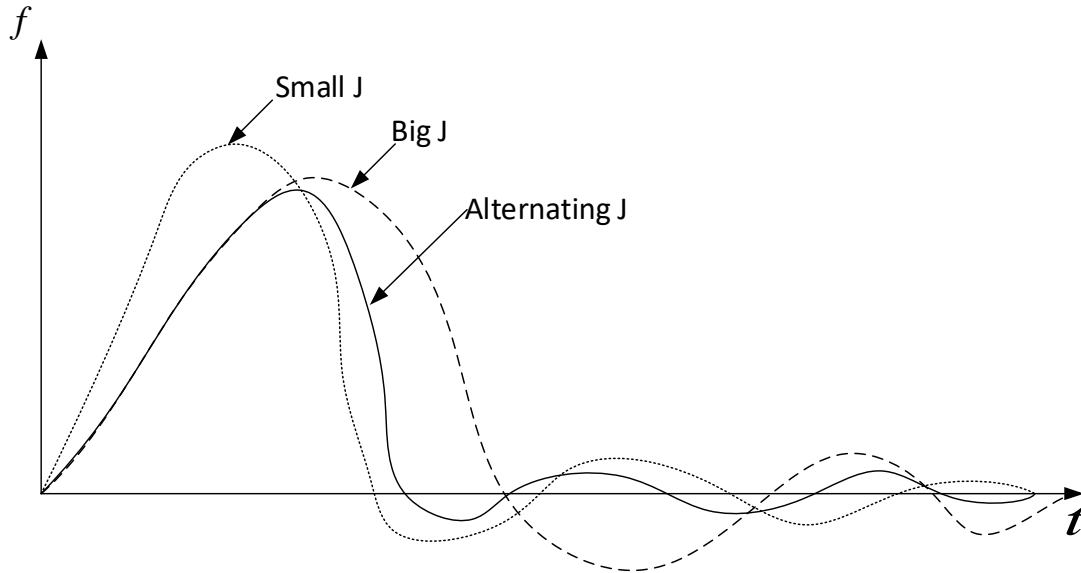
Figure 3.3 The ideal step response of the frequency for alternating inertia

For those four segments, the control strategy can be summarized as the following table:

Table 3.1 Alternating Inertia During the System Oscillation

$\Delta\omega$	$d\omega_{vsg}/dt$	Status	Alternating J
$\Delta w > 0$	$d\omega_{vsg}/dt > 0$	Accelerating	Big J
$\Delta\omega > 0$	$d\omega_{vsg}/dt < 0$	Decelerating	Small J
$\Delta\omega < 0$	$d\omega_{vsg}/dt < 0$	Accelerating	Big J
$\Delta\omega < 0$	$d\omega_{vsg}/dt > 0$	Decelerating	Small J

This can be verified as follows:
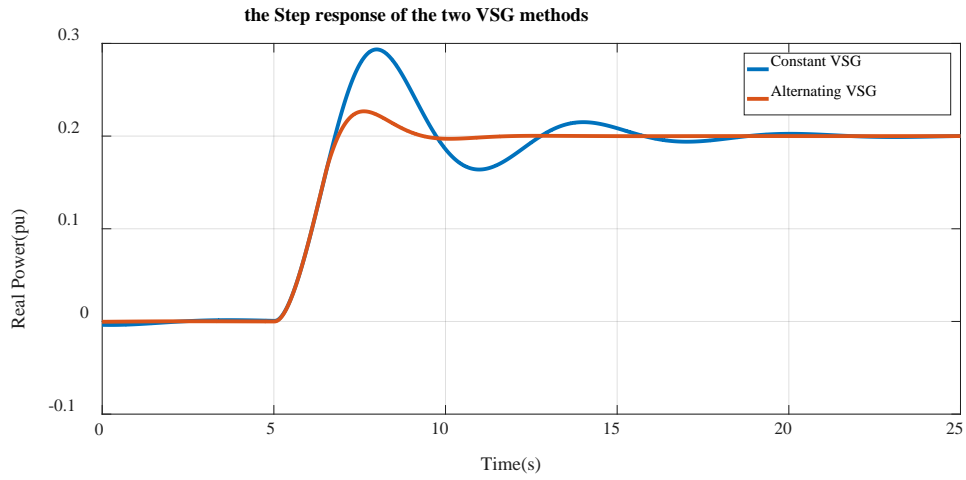
Figure 3.4 The Step response of the Real power of the two VSG methods
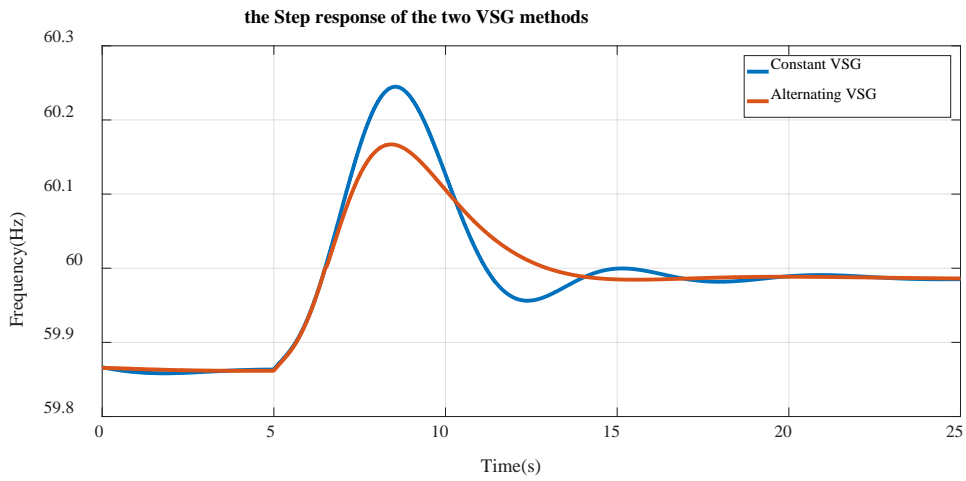
Figure 3.5 The Step response of the Frequency of the two VSG methods
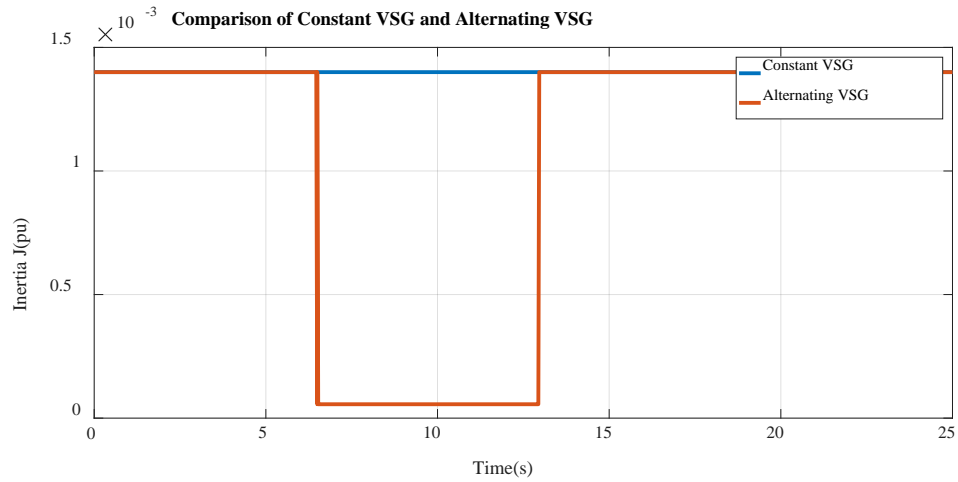
Figure 3.6 The Comparison of the two VSG methods

Here, at time t=5s, the step power reference of 0.2 pu is set for the BESS-VSG, and

we can see both the real power and the frequency response can be stable by using the VSG

methods. However, the Alternating VSG method has better performance than the Constant

VSG method with smaller overshooting and settling time.

Chapter Four: Case Study

4.1 System Structure and Scale

The model of the system is built in MATLAB/Simulink, which is shown as below:
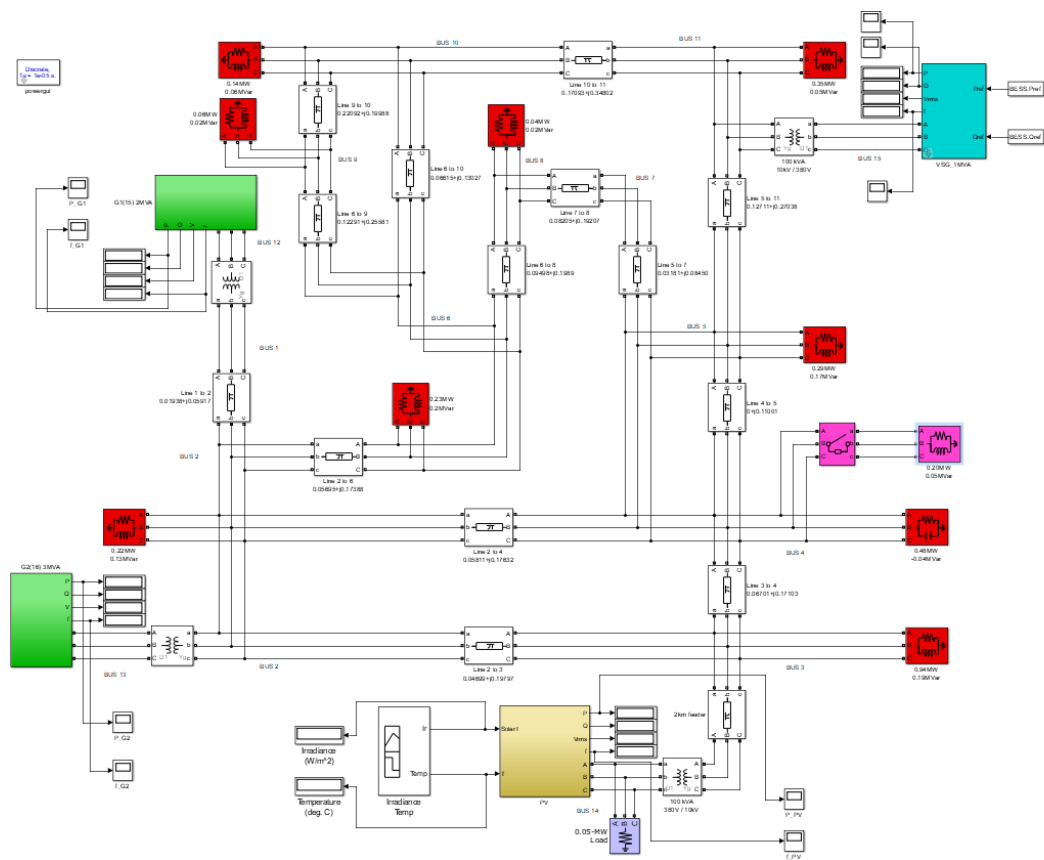
Figure 4.1 The overall model of the system in MATLAB/Simulink

In the diagram, the two green blocks represent the two traditional synchronous

generators G1 and G2; the yellow one represents the PV system; the cyan one represents

the BESS-VSG system; and those red blocks represent the loads. Inside the PV block, there are MPPT and Voltage Source Converter (VSC), which work together to meet the requirement. The diagram is shown as below:
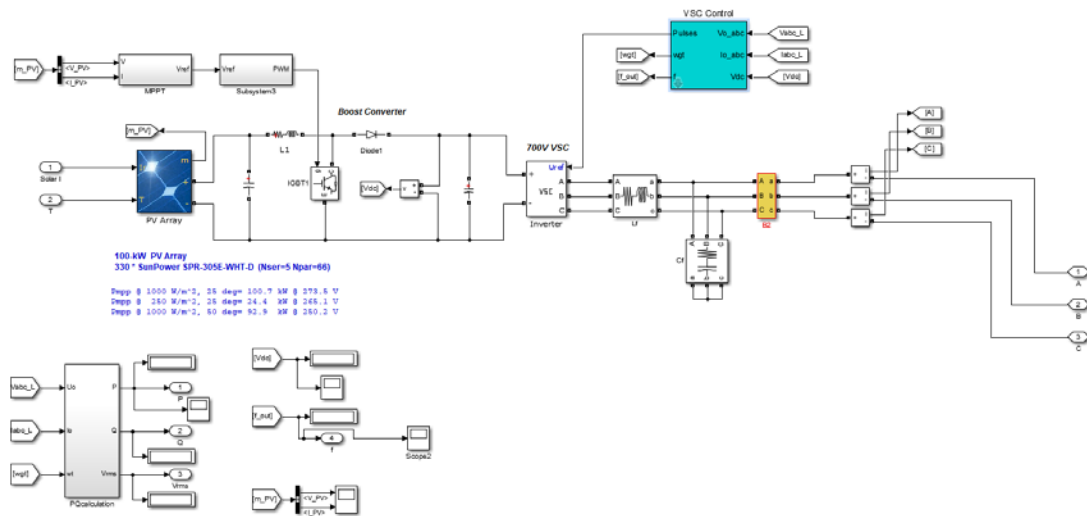
Figure 4.2 The diagram of PV subsystem

Besides, the BESS-VSG diagram is shown:
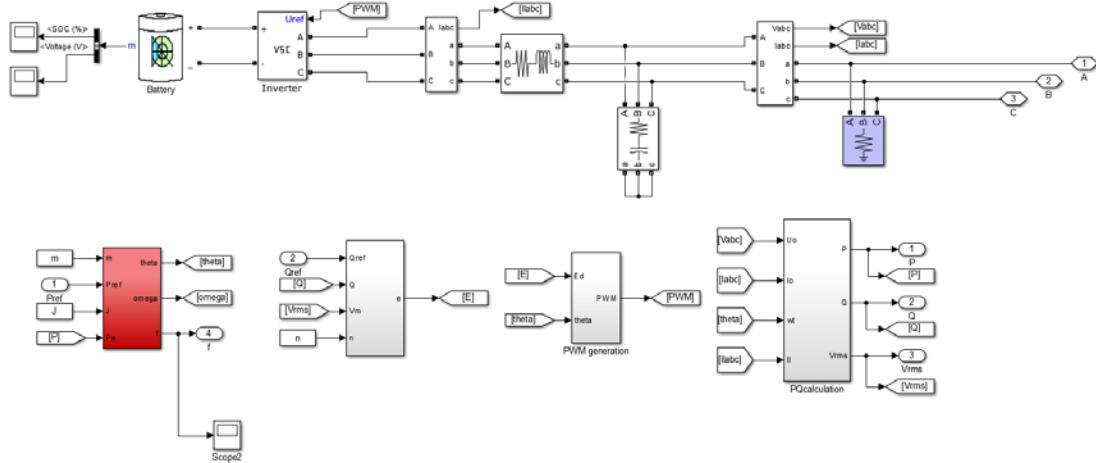
Figure 4.3 The diagram of BESS-VSG subsystem

And the parameters of the entire system are listed in the following table:

Table 4.1 The power of generations and loads

Bus Number	Type	Real Power (MW)	Reactive Power (MVar)
Bus 1	Generation	Inf	Inf
Bus 2	Load	0.22	0.13
Bus 3	Load	0.94	0.19
Bus 4	Load	0.48	-0.04
Bus 4	Break/Load	0.20	0.05
Bus 5	Load	0.29	0.17

Bus 6	Load	0.23	0.20
Bus 7	/	0	0
Bus 8	Load	0.04	0.02
Bus 9	Load	0.06	0.02
Bus 10	Load	0.14	0.06
Bus 11	Load	0.35	0.05
Bus 12	Generator1	1.46	0.29
Bus 13	Generator2	1.50	0.47
Bus 14	PV	0.10	0
Bus 14	Load	0.05	0
Bus 15	BESS-VSG	0.20	0

where, the infinity power supply only exists in the case when an infinite bus from a strong grid exists. In the cases that show the performance of VSG for frequency adjustment, the infinity power supply will be removed.

And the line parameters are shown as in the following table:

Table 4.2 The line parameters between different buses

Bus No.	Impedance (Ohm)
Bus 1-2	0.01938+j0.05917
Bus 2-3	0.04699+j0.19797
Bus 2-4	0.05811+j0.17632
Bus 2-6	0.05695+j0.17388
Bus 3-4	0.06701+j0.17103
Bus 4-5	0+j0.11001
Bus 5-7	0.03181+j0.08450
Bus 5-11	0.12711+j0.27038
Bus 6-8	0.09498+j0.1989
Bus 6-9	0.12291+j0.25581
Bus 6-10	0.06615+j0.13027
Bus 7-8	0.08205+j0.19207
Bus 9-10	0.22092+j0.19988
Bus 10-11	0.17093+j0.34802

And parameters of the transformers are listed as below:

Table 4.3 The parameters of the transformers between different buses

Bus No.	High Side (V)	Low Side (V)
Bus 1-12	22e3	10e3
Bus 2-13	13.8e3	10e3
Bus 3-14	10e3	380
Bus 11-15	10e3	380

4.2 Simulation Results

4.2.1 Case 1 (Grid-connected mode with constant irradiance and temperature)

First, the PV-grid-connected system is tested with constant irradiance and temperature. Based on this basic case, the whole system is proved normal and stable, then it can be modified for later cases. The simulation results are shown as below:
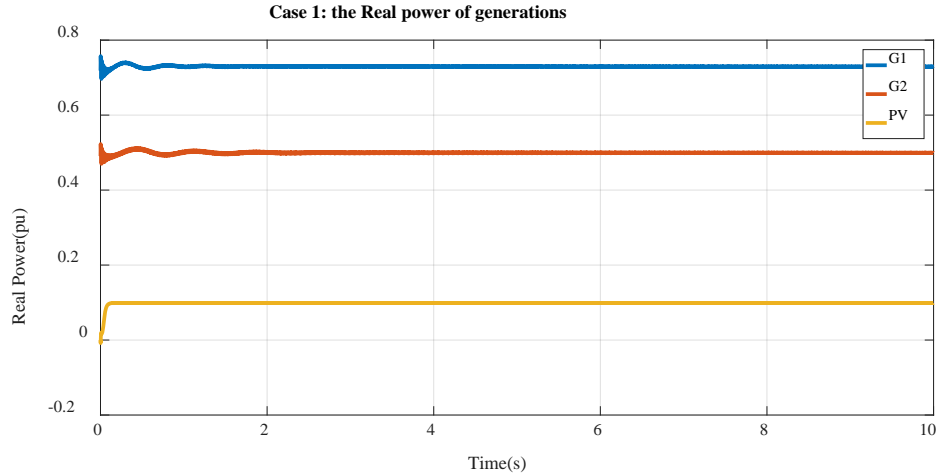
Figure 4.4 The real power of generations for Case 1
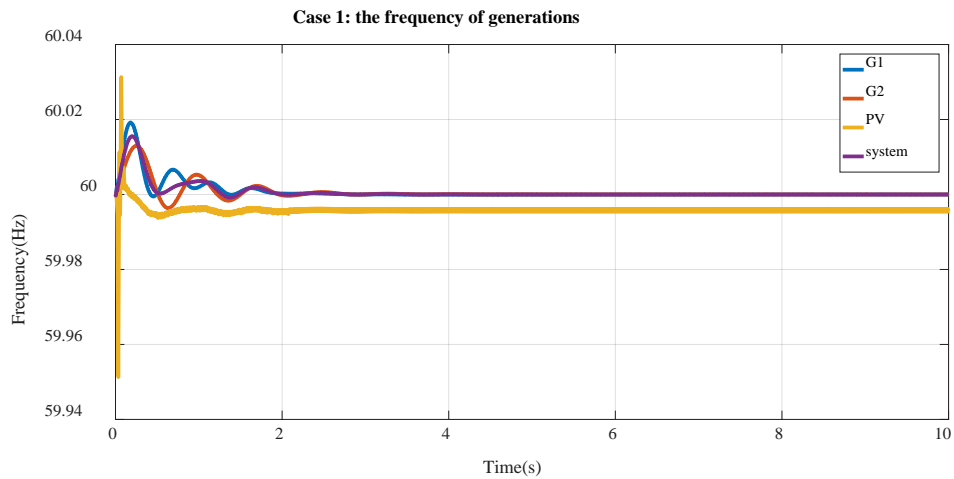
Figure 4.5 The frequency of generations for Case 1

From the figures, it can be seen that the system reaches the stable state very fast due

to the proper parameters of corresponding controllers. And the real power of G1 maintains

at about 0.73 pu, which is 1.46 MW because the base power for G1 is 2 MW. G2 maintains

about at 0.5 pu, which is 1.5 MW with its base power of 3MW. PV system outputs the

maximum power about at 0.1 MW constantly with the constant irradiance and temperature.

In addition, the frequencies of all sources are kept at 60 Hz steadily.

4.2.2 Case 2 (Grid-connected mode with varying irradiance and temperature)

The difference between the Case 1 and Case 2 is the varying irradiance and

temperature for the PV system. The aim is to verify the robustness of the MPPT control of

the PV system. That is to say, the PV system can output the maximum power constantly

even though there is fluctuation in the weather. The irradiance and the temperature signals

are built by a signal builder as below:
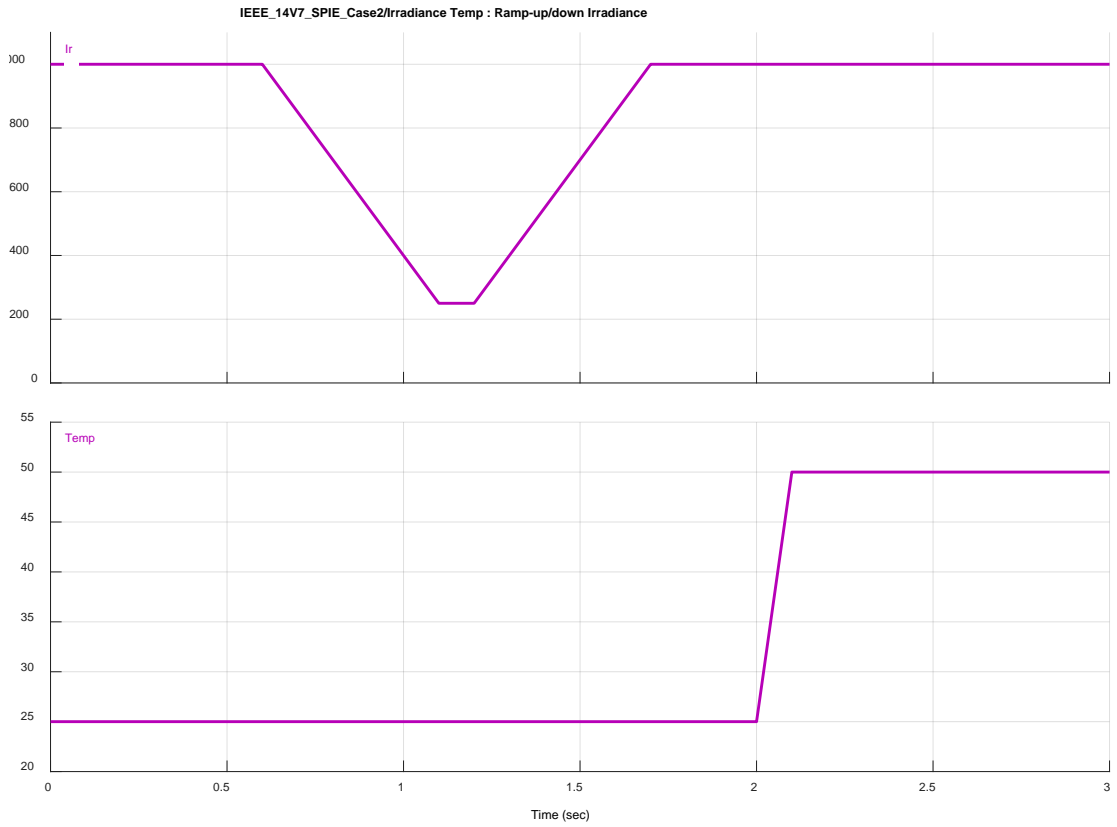
Figure 4.6 The varying irradiance and temperature signals for Case 2

The results are shown as below:
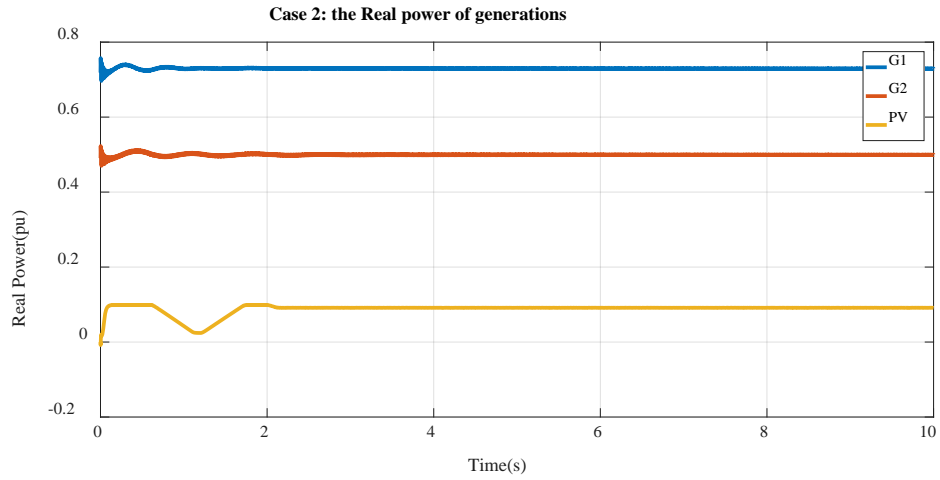
Figure 4.7 The real power of generations for Case 2
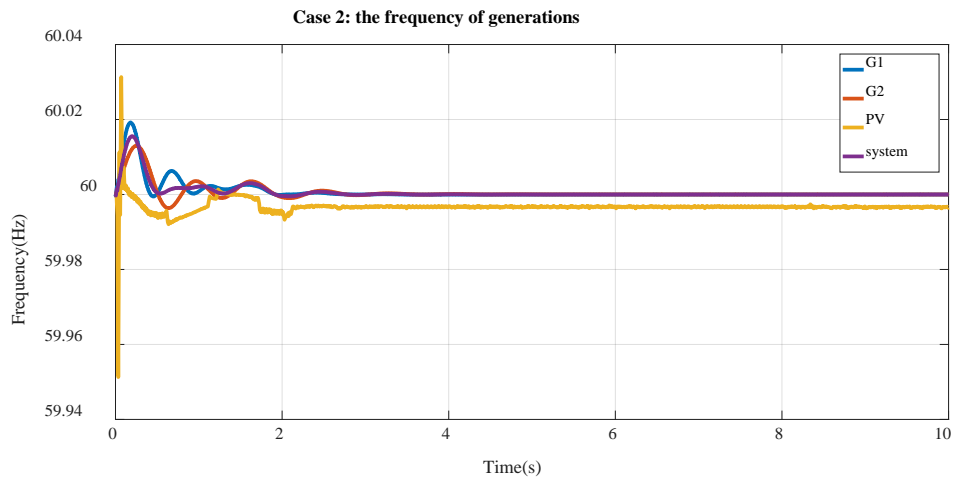
Figure 4.8 The frequency of generations for Case 2

Different from Case 1, the real power generated by PV system is decreased as the

irradiance decreases and temperature increases at about time 0.6s and 2.0s respectively,

and then it returns to the normal value. The corresponding phenomenon can also be seen in the frequency figure.

4.2.3 Case 3 (Grid-connected mode to Islanded mode)

Case 3 shows the transients from the grid-connected mode to islanded mode. In this case, the circuit break between the infinite power supply and the lines is set to be closed at time 0s, opened at time 3s. The results are shown as below:

Figure 4.9 The real power of generations of Case 3

51
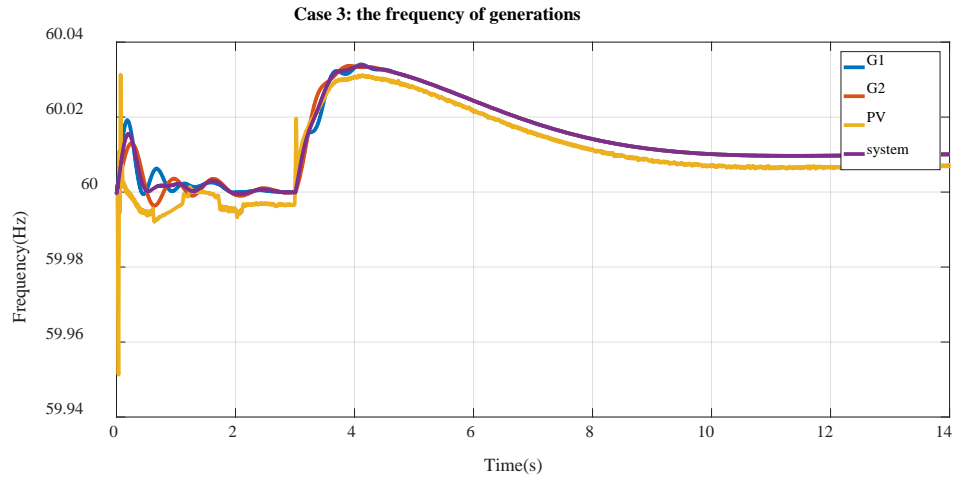
Figure 4.10 The frequency of generations of Case 3

It can be seen that from time 0s to time 3s, the system is running at grid-connected

mode, and it is stable. Then, at time 3s, the real power and frequency of each generation

have a little fluctuation because the main power supply is removed, but the system finally

reaches stable state. Therefore, both grid-connected and islanded mode are proved to be

stable for this system.

4.2.4 Case 4 (Islanded mode: load increases without VSG)

Case 4 is for in islanded mode operation, and the aim is to observe how frequency

changes when the load increases without any extra generation. The results are shown as

below:
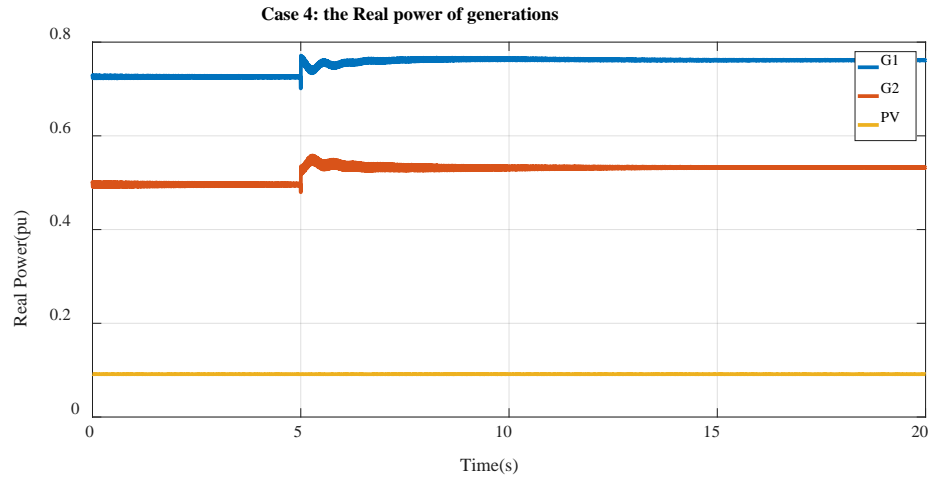
Figure 4.11 The real power of generations of Case 4
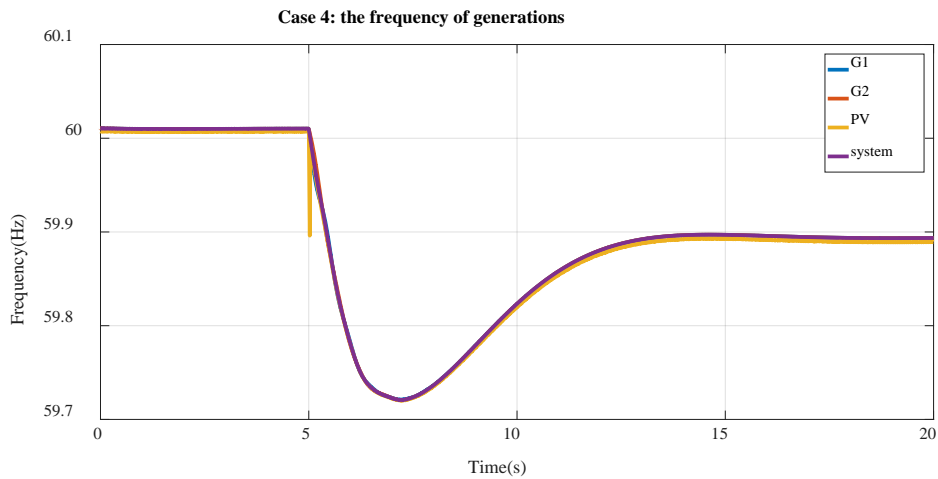
Figure 4.12 The frequency of generations of Case 4

In this case, at time 5s, there is a load increase with 0.2 MW, 0.05 MVar. From the

figures, it can be seen that the synchronous generators increase their generations because

of the inherent characteristic of the traditional power system. However, it is not enough to

balance the increased load. Then the frequency decreases suddenly, and the slope in this period is very steep. The lowest frequency approaches to about 59.72 Hz, which is harmful to the power system. Finally, under the coordination of generators and loads, the system is running at a new stable point, but the frequency is lower than 60 Hz. This is also the reason why the VSG technique is used to track the system back to the original state.

4.2.5 Case 5 (Islanded mode: load increases with constant VSG)

Based on Case 4, the VSG is added to supply the increased load. VSG inertia $J = 1.4 \times 10^{-3} pu$ results in very good performance and the results are shown as below:
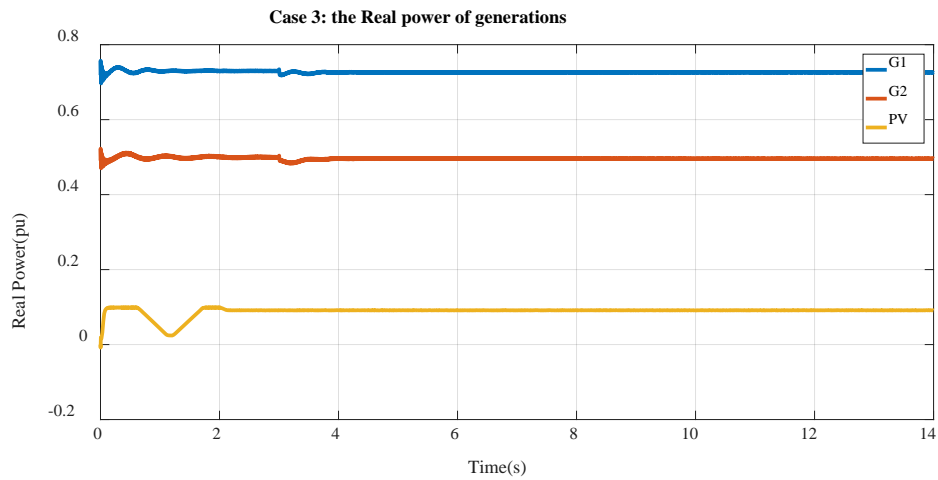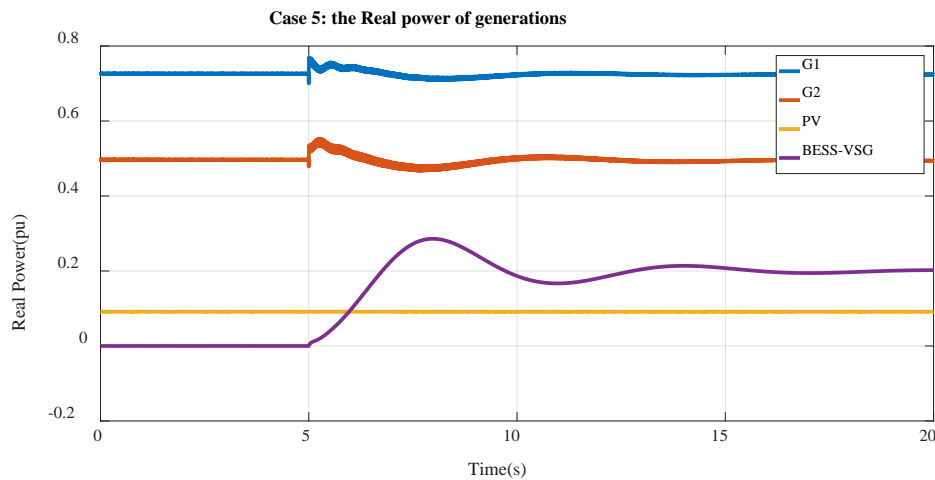

Figure 4.13 The real power of generations of Case 5
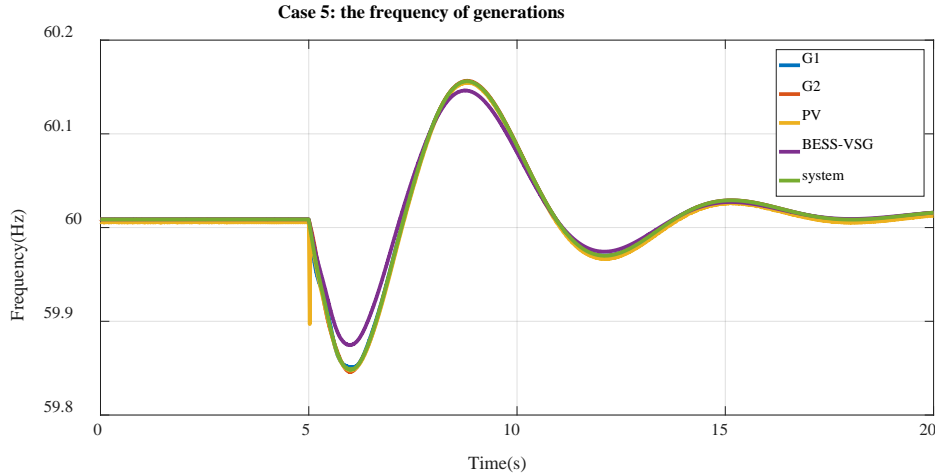
Figure 4.14 The frequency of generations of Case 5

It can be seen that for the same condition, with the BESS-VSG technique, the lowest

point of the frequency is about 59.85 Hz when the load increases, which is allowable in

real power system. Finally, the system is running at a new stable point at frequency about

60.01 Hz.

4.2.5 Case 6 (Islanded mode: load increases with alternating VSG)

In order to enhance the performance of making the frequency drop curve smoother,

the alternating VSG technique is used in the same condition with Case 4 and Case 5. And

the $Big\ J = 1.4 \times 10^{-3} pu,\ Small\ J = 5.62 \times 10^{-5} pu$ The results are shown as below:
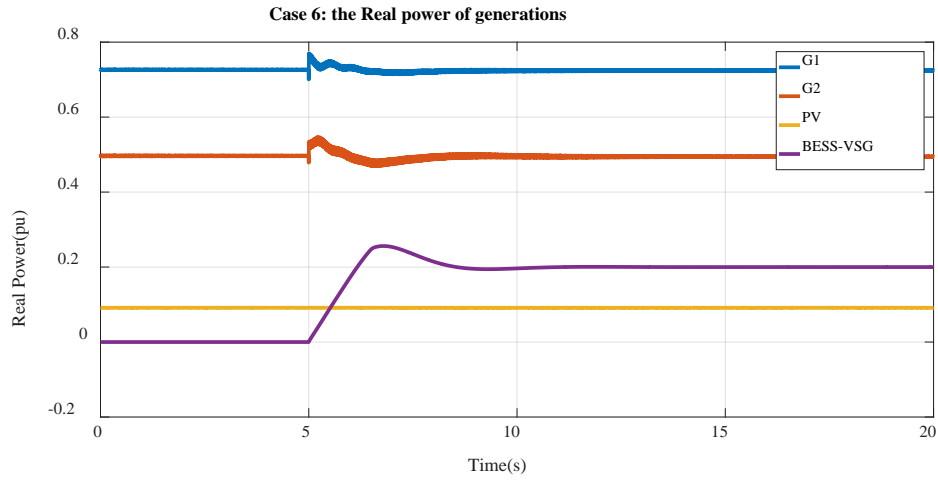
Figure 4.15 The real power of generations of Case 6 with alternating J
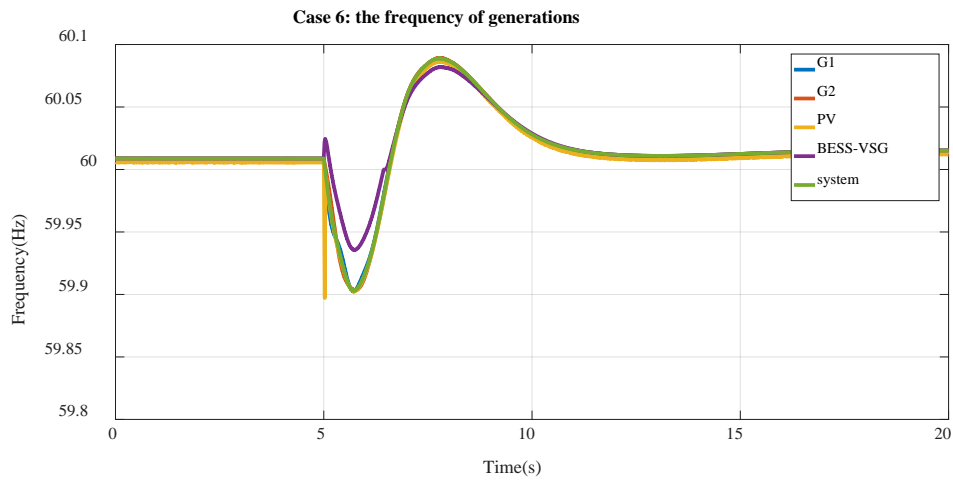
Figure 4.16 The frequency of generations of Case 6 with alternating J

To observe the improvement of the performance directly, comparison between the results of the constant VSG and the alternating VSG are shown as below:
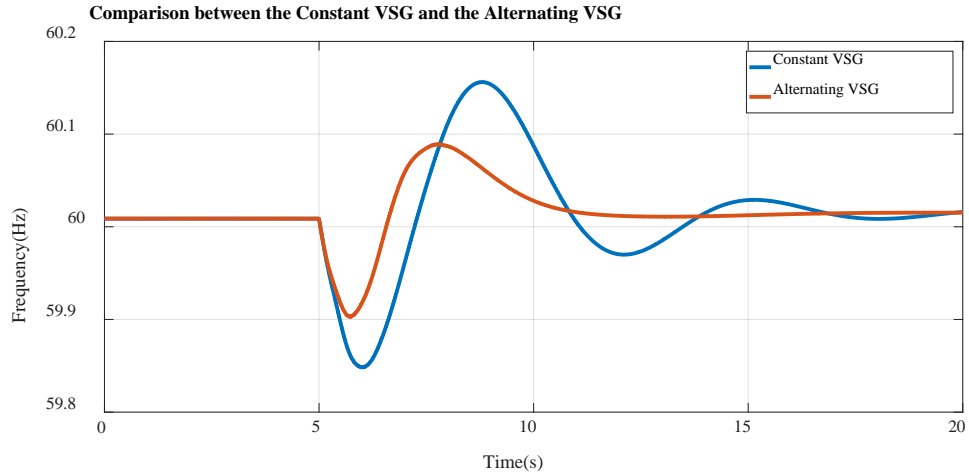
Figure 4.17 The comparison between the Constant VSG and the Alternating VSG

And for convenience, those results can be summarized as the following table:

Table 4.4 Summary of these six cases

Case1: Grid-connected mode (Constant solar irradiation and temperature)	Stable with frequency at 60Hz
Case2: Grid-connected mode (Variable solar irradiation and temperature)	Stable with frequency at 60Hz
Case3: Grid-connected mode to Islanded mode	Stable with frequency at 60.01Hz
Case4: Load increases in Islanded mode without VSG	Stable with frequency at 59.9Hz

Case5: Load increases in Islanded mode with Constant VSG	Stable with frequency at 60.01Hz
Case6: Load increases in Islanded mode with Alternating VSG	Stable with frequency at 60.01Hz and smaller overshooting, settling time

4.3 Discussion

By analyzing and comparing the results of the six case studies, the following conclusions can be obtained:

1. By using MPPT controller, the PV system can output the maximum power no matter whether the irradiance and temperature are constant or varying.

2. By using the traditional dual loop control including voltage outer loop and current inner loop for inverter, the system can work well in either grid-connected mode or islanded mode.

3. Case 5 reflects the successful VSG controller for the system when the load increases, in which the frequency and voltage can be controlled within an allowable range.

4. Case 6 indicates that the alternating VSG controller has better performance than constant VSG controller in making the frequency drop curve smoother when the load increases suddenly.

Chapter Five: Conclusions and Future Work

5.1 Conclusions

Solving frequency control problem is the most important way to guarantee the stability of microgrid power system. Also, renewable energy such as PV is more and more popular in today's power system. This thesis aims to make the PV based microgrid behavior like a traditional power system during islanded mode operation. The frequency stability performance is enhanced by a proposed Alternating VSG method. With respect to the contributions, the conclusions of this thesis are given as follows:

1. The PV system maximizes its performance by using the P&O MPPT Algorithm under changing weather conditions.

2. The PV based microgrid system is synchronous with the grid based on the same frequency due to the double loop controller for inverter and it can run in either grid-connected mode or islanded mode.

3. The proposed VSG technique can alleviate the frequency dip problem due to load increase, thereby guarantee the quality of the electricity.

4. By using the Alternating VSG technique, the performance is further improved, which is innovative and significant to the area of power system stability control.

5.2 Future Work

The frequency control of the small scale microgrid are verified by simulation in this thesis, and an advanced method for frequency stability is proposed. However, there are still some future work that are needed to be continued:

1. For some microgrids, there may be some other renewable resources, such as wind turbines. A wind turbine control including region 2, region 3 and grid-connected control will be added in the future simulation.

2. For realistic applications, a larger scale microgrid including communication between each subsystem is more complex. Therefore, several PV, wind turbine and battery storage systems will be added to the existing model, and a distributed cooperative control needs to be implemented considering communication and physical structures.

3. In this thesis, all the case studies are analyzed in MATLAB/Simulink; however, there are some implementation issues which cannot be shown in simulation. Therefore, a Hardware-in-the-Loop (HILP) will be implemented in the future work, which can mimic the response of the real power system based on Real Time Digital Simulator (RTDS).

Reference

[1] R. H. Lasseter, "MicroGrids," 2002 IEEE Power Engineering Society Winter Meeting. Conference Proceedings (Cat. No.02CH37309), New York, NY, USA, 2002, pp. 305-308 vol.1.

[2] Department of Energy Office of Electricity Delivery and Energy Reliability. (2012). Summary Report: 2012 DOE Microgrid Workshop. [Online]. Available: http://energy.gov/sites/prod/files/2012%20Microgrid%20Workshop%20Report%2009 102012.pdf, accessed Nov. 13, 2014.

[3] Lasseter R H, Piagi P. "Control and design of microgrid components[J]," PSERC Publication 06, 2006, 3.

[4] B. Yu, J. Guo, C. Zhou, Z. Gan, J. Yu and F. Lu, "A Review on Microgrid Technology with Distributed Energy," 2017 International Conference on Smart Grid and Electrical Automation (ICSGEA), Changsha, 2017, pp. 143-146.

[5] J. A. P. Lopes et al., "Control strategies for microgrids emergency operation," 2005 International Conference on Future Power Systems, Amsterdam, 2005, pp. 6 pp.-6.

[6] M. C. Chandorkar, D. M. Divan and R. Adapa, "Control of parallel connected inverters in standalone AC supply systems," in IEEE Transactions on Industry Applications, vol. 29, no. 1, pp. 136-143, Jan.-Feb. 1993.

[7] Li, Y., Zhang, H., Huang, B. et al. A distributed Newton–Raphson-based coordination algorithm for multi-agent optimization with discrete-time communication. Neural Comput & Applic (2018). https://doi.org/10.1007/s00521-018-3798-1

[8] Li, Y., Zhang, H., Han, J., & Sun, Q. (2018). Distributed multi-agent optimization via event-triggered based continuous-time Newton-Raphson algorithm. Neurocomputing, 275, 1416-1425.

[9] Y. Li, H. Zhang, X. Liang and B. Huang, "Event-Triggered-Based Distributed Cooperative Energy Management for Multienergy Systems," in IEEE Transactions on Industrial Informatics, vol. 15, no. 4, pp. 2008-2022, April 2019.

[10] Z. Mingsheng, F. Peilei, W. Hesong, W. Wenkui and C. Pengcheng, "Hierarchical Control Strategy for Microgrid," 2018 2nd IEEE Advanced Information Management,Communicates,Electronic and Automation Control Conference (IMCEC), Xi'an, 2018, pp. 1528-1532.

[11] W. Yan, D. W. Gao, F. Zhang, L. Cheng and S. Yan, "Modeling and analysis of secondary controlled virtual synchronous generator with dynamic droop for

microgrid," 2017 IEEE Conference on Energy Internet and Energy System Integration (EI2), Beijing, 2017, pp. 1-6.

[12] Mohammad Dreidy, H. Mokhlis, Saad Mekhilef, "Inertia response and frequency control techniques for renewable energy sources: A review," Renewable and Sustainable Energy Reviews, Volume 69, 2017, Pages 144-155.

[13] T. Kerdphol, F. S. Rahman, M. Watanabe and Y. Mitani, "Robust Virtual Inertia Control of a Low Inertia Microgrid Considering Frequency Measurement Effects," in IEEE Access, vol. 7, pp. 57550-57560, 2019.

[14] J. Driesen and K. Visscher, "Virtual synchronous generators," 2008 IEEE Power and Energy Society General Meeting - Conversion and Delivery of Electrical Energy in the 21st Century, Pittsburgh, PA, 2008, pp. 1-3.

[15] Q. Zhong and G. Weiss, "Synchronverters: Inverters That Mimic Synchronous Generators," in IEEE Transactions on Industrial Electronics, vol. 58, no. 4, pp. 1259-1267, April 2011.

[16] W. Yan, W. Gao, T. Gao, D. W. Gao, S. Yan and J. Wang, "Distributed cooperative control of virtual synchronous generator based microgrid," 2017 IEEE International Conference on Electro Information Technology (EIT), Lincoln, NE, 2017, pp. 506-511.

[17] W. Yan, D. Wenzhong Gao and S. Huang, "Distributed Secondary Control of Virtual Synchronous Generator Integrated Microgrid via Extremum Seeking," 2018 IEEE/PES Transmission and Distribution Conference and Exposition (T&D), Denver, CO, 2018, pp. 1-5.

[18] Z. Wu, D. W. Gao, T. Gao, W. Yan, H. Zhang, S. Yan, and X. Wang, "State-of-the-art review on frequency response of wind power plants in power systems," Journal of Modern Power Systems, vol. 6, no.1, pp. 1-16, Jan 2018.

[19] W. Yan, L. Cheng, S. Yan, W. Gao and W. Gao, "Enabling and Evaluation of Inertial Control for PMSG-WTG using Synchronverter with Multiple Virtual Rotating Masses in Microgrid," in IEEE Transactions on Sustainable Energy.

[20] Yan, X. & Liu, Z. & Zhang, B. & Lü, Z. & Su, X. & Xu, H. & Ren, Y.. (2016), "Small-signal stability analysis of parallel inverters with synchronous generator characteristics," 40. 910-917. 10.13335/j.1000-3673.pst.2016.03.036.

[21] Ise, Toshifumi & Bevrani, H.. (2016), "Virtual synchronous generators and their applications in microgrids," 10.1016/B978-0-12-803212-1.00012-X.

[22] Salvatore D'Arco, Jon Are Suul, Olav B. Fosso, "A Virtual Synchronous Machine implementation for distributed control of power converters in SmartGrids," Electric Power Systems Research, Volume 122, 2015, Pages 180-197.

[23] M. Suthar, G. K. Singh and R. P. Saini, "Comparison of mathematical models of photo-voltaic (PV) module and effect of various parameters on its performance," 2013 International Conference on Energy Efficient Technologies for Sustainability, Nagercoil, 2013, pp. 1354-1359.

[24] Tsai, Huan-Liang & Ci-Siang, Tu & Yi-Jie, Su. (2008), "Development of generalized photovoltaic model using MATLAB/SIMULINK," Lecture Notes in Engineering and Computer Science. 2173.

[25] Chihchiang Hua and Chihming Shen, "Study of maximum power tracking techniques and control of DC/DC converters for photovoltaic power system," PESC 98 Record. 29th Annual IEEE Power Electronics Specialists Conference (Cat. No.98CH36196), Fukuoka, 1998, pp. 86-93 vol.1.

[26] C. Chang, J. Zhu and H. Tsai, "Model-based performance diagnosis for PV systems," Proceedings of SICE Annual Conference 2010, Taipei, 2010, pp. 2139-2145.

[27] Z. Salam, K. Ishaque and H. Taheri, "An improved two-diode photovoltaic (PV) model for PV system," 2010 Joint International Conference on Power Electronics, Drives and Energy Systems & 2010 Power India, New Delhi, 2010, pp. 1-5.

[28] Weidong Xiao and W. G. Dunford, "A modified adaptive hill climbing MPPT method for photovoltaic power systems," 2004 IEEE 35th Annual Power Electronics Specialists

Conference (IEEE Cat. No.04CH37551), Aachen, Germany, 2004, pp. 1957-1963 Vol.3.

[29] Eltamaly, Ali & Rezk, Hegazy. (2015), "A comprehensive comparison of different MPPT techniques for photovoltaic systems," Solar Energy. 112. 1-11. 10.1016/j.solener.2014.11.010.

[30] F. Liu, S. Duan, F. Liu, B. Liu and Y. Kang, "A Variable Step Size INC MPPT Method for PV Systems," in IEEE Transactions on Industrial Electronics, vol. 55, no. 7, pp. 2622-2628, July 2008.

[31] Eltamaly, Ali. (2010), "Modeling of Fuzzy Logic Controller for Photovoltaic Maximum Power Point Tracker."

[32] Yusof, Yushaizad & Sayuti, S.H. & Latif, Md & Wanik, M.Z.C.. (2004), "Modeling and simulation of maximum power point tracker for photovoltaic system," 88 - 93. 10.1109/PECON.2004.1461622.

[33] E. Koutroulis, K. Kalaitzakis and N. C. Voulgaris, "Development of a microcontroller-based, photovoltaic maximum power point tracking control system," in IEEE Transactions on Power Electronics, vol. 16, no. 1, pp. 46-54, Jan. 2001.

[34] T. Esram and P. L. Chapman, "Comparison of Photovoltaic Array Maximum Power Point Tracking Techniques," in IEEE Transactions on Energy Conversion, vol. 22, no. 2, pp. 439-449, June 2007.

[35] Chengshan Wang, "Analysis and Simulation Theory of Microgrids," 2013.

[36] Y. Xu and C. Singh, "Distribution systems reliability and economic improvement with different electric energy storage control strategies," 2011 IEEE Power and Energy Society General Meeting, Detroit, MI, USA, 2011, pp. 1-8.

[37] A. M. Massoud, S. Ahmed, S. J. Finney and B. W. Williams, "Inverter-based versus synchronous-based distributed generation; fault current limitation and protection issues," 2010 IEEE Energy Conversion Congress and Exposition, Atlanta, GA, 2010, pp. 58-63.

[38] X. Xiaofei, L. Hong and L. Zhipeng, "Research on new algorithm of droop control," 2018 Chinese Control And Decision Conference (CCDC), Shenyang, 2018, pp. 4166-4170.

[39] L. Jia, C. Du, C. Zhang and A. Chen, "An improved droop control method for reducing current sensors in DC microgrid," 2017 Chinese Automation Congress (CAC), Jinan, 2017, pp. 4645-4649.

[40] F. Alam, M. Ashfaq, S. S. Zaidi and A. Y. Memon, "Robust droop control design for a hybrid AC/DC microgrid," 2016 UKACC 11th International Conference on Control (CONTROL), Belfast, 2016, pp. 1-6.

[41] Zhou, XueSong & Guo, Tie & Ma, YouJie. (2017), "An Overview on Operation and Control of Microgrid," DEStech Transactions on Engineering and Technology Research. 10.12783/dtetr/mcee2016/6412.

[42] Yang, Z. & Wang, C. & Che, Y.. (2009), "A small-scale microgrid system with flexible modes of operation," 33. 89-92+98.

[43] Brabandere, Karel De. "Voltage and Frequency Droop Control in Low Voltage Grids by Distributed Generators with Inverter Front-End," (2006).

[44] J. M. Guerrero, L. G. de Vicuna, J. Matas, M. Castilla and J. Miret, "A wireless controller to enhance dynamic performance of parallel inverters in distributed generation systems," in IEEE Transactions on Power Electronics, vol. 19, no. 5, pp. 1205-1213, Sept. 2004.

[45] H. Laaksonen, P. Saari and R. Komulainen, "Voltage and frequency control of inverter based weak LV network microgrid," 2005 International Conference on Future Power Systems, Amsterdam, 2005, pp. 6 pp.-6.

[46] F. Blaabjerg, R. Teodorescu, M. Liserre and A. V. Timbus, "Overview of Control and Grid Synchronization for Distributed Power Generation Systems," in IEEE Transactions on Industrial Electronics, vol. 53, no. 5, pp. 1398-1409, Oct. 2006.

[47] A. V. Timbus, R. Teodorescu, F. Blaabjerg, M. Liserre and A. Dell'Aquila, "Independent synchronization and control of three phase grid converters," International Symposium on Power Electronics, Electrical Drives, Automation and Motion, 2006. SPEEDAM 2006., Taormina, 2006, pp. 1246-1251.

[48] S. M. Silva, B. M. Lopes, B. J. C. Filho, R. P. Campana and W. C. Bosventura, "Performance evaluation of PLL algorithms for single-phase grid-connected systems," Conference Record of the 2004 IEEE Industry Applications Conference, 2004. 39th IAS Annual Meeting., Seattle, WA, USA, 2004, pp. 2259-2263 vol.4.

[49] R. M. Santos Filho, P. F. Seixas, P. C. Cortizo, L. A. B. Torres and A. F. Souza, "Comparison of Three Single-Phase PLL Algorithms for UPS Applications," in IEEE Transactions on Industrial Electronics, vol. 55, no. 8, pp. 2923-2932, Aug. 2008.

[50] P. Sindhuja and V. U. Reddy, "Enhancement of grid connected PV inverter using optimal maximum power point tracking algorithm with estimation of climatic parameter," 2017 International Conference on Inventive Systems and Control (ICISC), Coimbatore, 2017, pp. 1-6.

[51] M. Liserre, T. Sauter and J. Y. Hung, "Future Energy Systems: Integrating Renewable Energy Sources into the Smart Power Grid Through Industrial Electronics," in IEEE Industrial Electronics Magazine, vol. 4, no. 1, pp. 18-37, March 2010.

[52] Bevrani, H. & Ise, Toshifumi & Miura, Yushi. (2014), "Virtual synchronous generators: A survey and new perspectives," International Journal of Electrical Power & Energy Systems. 54. 244-254. 10.1016/j.ijepes.2013.07.009.

[53] J. Liu, Y. Miura, H. Bevrani and T. Ise, "Enhanced Virtual Synchronous Generator Control for Parallel Inverters in Microgrids," in IEEE Transactions on Smart Grid, vol. 8, no. 5, pp. 2268-2277, Sept. 2017.

[54] Q. Zhong, "Virtual Synchronous Machines: A unified interface for grid integration," in IEEE Power Electronics Magazine, vol. 3, no. 4, pp. 18-27, Dec. 2016.

[55] M. Mao, C. Qian and Y. Ding, "Decentralized coordination power control for islanding microgrid based on PV/BES-VSG," in CPSS Transactions on Power Electronics and Applications, vol. 3, no. 1, pp. 14-24, March 2018.

[56] O. Tremblay, L. Dessaint and A. Dekkiche, "A Generic Battery Model for the Dynamic Simulation of Hybrid Electric Vehicles," 2007 IEEE Vehicle Power and Propulsion Conference, Arlington, TX, 2007, pp. 284-289.

[57] Songrang Zhu, "Lead Acid Battery Technology[M]," 2002.

[58] Y. Xiang-zhen, S. Jian-hui, D. Ming, L. Jin-wei and D. Yan, "Control strategy for virtual synchronous generator in microgrid," 2011 4th International Conference on Electric Utility Deregulation and Restructuring and Power Technologies (DRPT), Weihai, Shandong, 2011, pp. 1633-1637.

[59] J. Alipoor, Y. Miura and T. Ise, "Power System Stabilization Using Virtual Synchronous Generator With Alternating Moment of Inertia," in IEEE Journal of Emerging and Selected Topics in Power Electronics, vol. 3, no. 2, pp. 451-458, June 2015.